Chemical Geology 532 (2020) 119324

Contents lists available at ScienceDirect

Chemical Geology

journal homepage: www.elsevier.com/locate/chemgeo

Invited Research Article

The multiple depleted mantle components in the Hawaiian-Emperor chain

Lauren N. Harrison[a,b,*], Dominique Weis[a], Michael O. Garcia[c]

[a] Pacific Centre for Isotopic and Geochemical Research, Department of Earth, Ocean, and Atmospheric Sciences, University of British Columbia, Vancouver, B.C., Canada
[b] Nuclear and Chemical Sciences, Lawrence Livermore National Lab, Livermore, CA, USA
[c] Department of Geology and Geophysics, University of Hawaii, Honolulu, HI, USA

ARTICLE INFO

Keywords:
Oceanic island basalts
Hawaiian-Emperor chain
Depleted components
Isotopes
Mantle geochemistry

ABSTRACT

Oceanic island basalts are targeted for geochemical study because they provide a direct window into mantle composition and a wealth of information on the dynamics and timescales associated with Earth mixing. Previous studies mainly focused on the shield volcanic stage of oceanic islands and the more fusible, enriched mantle components that are easily distinguished in those basalts. Mantle depleted compositions are typically more difficult to resolve unless large amounts of this material participated in mantle melting (e.g., mid-ocean ridges), or unique processes allow for their compositions to be erupted undiluted, such as very small degrees of melting of a source with minimal fusible enriched components (e.g., rejuvenated basalts) or as xenoliths (e.g., abyssal peridotites). Mantle depleted components, defined here as material with low time-integrated Rb/Sr (low $^{87}Sr/^{86}Sr$) and high time-integrated Sm/Nd and Lu/Hf ratios (high $^{143}Nd/^{144}Nd$ and $^{176}Hf/^{177}Hf$) relative to primitive mantle, derive from a potentially very large volume reservoir (up to 80% of the mantle), and therefore need adequate characterization in order estimate the composition of the Earth and mantle-derived melts. This review focuses on mantle depleted compositions in oceanic island basalts using the Hawaiian-Emperor chain as a case study. The Hawaiian-Emperor chain is the ~6000 km long geological record of the deeply sourced Hawaiian mantle plume, active for > 81 Myr. Hawaiian volcanism evolves through four volcanic stages as a volcano traverses the Hawaiian plume: alkalic preshield, tholeiitic shield (80–90% volcano volume), alkalic postshield (~1%), and silica undersaturated rejuvenated (< 0.1%). We report Pb-Sr-Nd-Hf isotope compositions and trace element concentrations of three rejuvenated Northwest Hawaiian Ridge basalts and compare them to an exhaustive compiled dataset of basalts from the Hawaiian Islands to the Emperor Seamounts. The Northwest Hawaiian Ridge (NWHR) includes 51 volcanoes spanning ~42 m.y. between the bend in the Hawaiian-Emperor chain and the Hawaiian Islands where there is no high-precision isotopic data published on the rejuvenated-stage over ~47% of the chain. NWHR and Hawaiian Island rejuvenated basalts are geochemically similar, indicating a consistent source for rejuvenated volcanism over ~12.5 million years. In contrast, shield-stage basalts from the oldest Emperor Seamounts are more depleted in isotopic composition (i.e., higher $^{176}Hf/^{177}Hf$, and $^{143}Nd/^{144}Nd$ with lower $^{87}Sr/^{86}Sr$ and $^{208}Pb^*/^{206}Pb^*$) and trace element concentrations (i.e., much lower concentrations of highly incompatible elements) than all other depleted Hawaiian basalts younger than the bend, including NWHR rejuvenated basalts. The strongly depleted source for the oldest Emperor Seamounts (> 70 Ma) was likely related to interaction with the Kula-Pacific-Izanagi mid-ocean ridge spreading system active near the Hawaiian plume in the Late Cretaceous. In contrast, the incompatible trace element ratios of NWHR rejuvenated basalts require a distinct source in the Hawaiian mantle plume that was imprinted by ancient (> 1 Ga) partial melting, likely ancient recycled oceanic lithosphere. This review of the geochemistry of Hawaiian depleted components documents the need for the sampling of multiple distinctive depleted compositions, each preferentially melted during specific periods of Hawaiian plume activity. This suggests that the composition of depleted components can evolve during the lifetime of the mantle plume, as observed for enriched components in the Hawaiian mantle plume. Changes in the composition of depleted components are dominantly controlled by the upper mantle tectonic configurations at the time of eruption (i.e., proximity to a mid-ocean ridge), as this effect overwhelms the signal imparted by potentially sampling different lower mantle components through time.

* Corresponding author at: Lawrence Livermore National Lab, Livermore, CA, USA.
E-mail address: harrison56@llnl.gov (L.N. Harrison).

https://doi.org/10.1016/j.chemgeo.2019.119324
Received 19 March 2019; Received in revised form 24 September 2019; Accepted 2 October 2019
Available online 24 October 2019
0009-2541/ Published by Elsevier B.V.

1. Introduction

The lower mantle is compositionally heterogeneous and dynamic over space and time (Hofmann, 2014; Garnero et al., 2016 and references therein). Global shear wave velocity tomography models show two thousand kilometer-wide, steep sided, and seismically-slow piles beneath the Pacific Ocean and continental Africa that are proposed reservoirs for incompatible element enriched recycled material

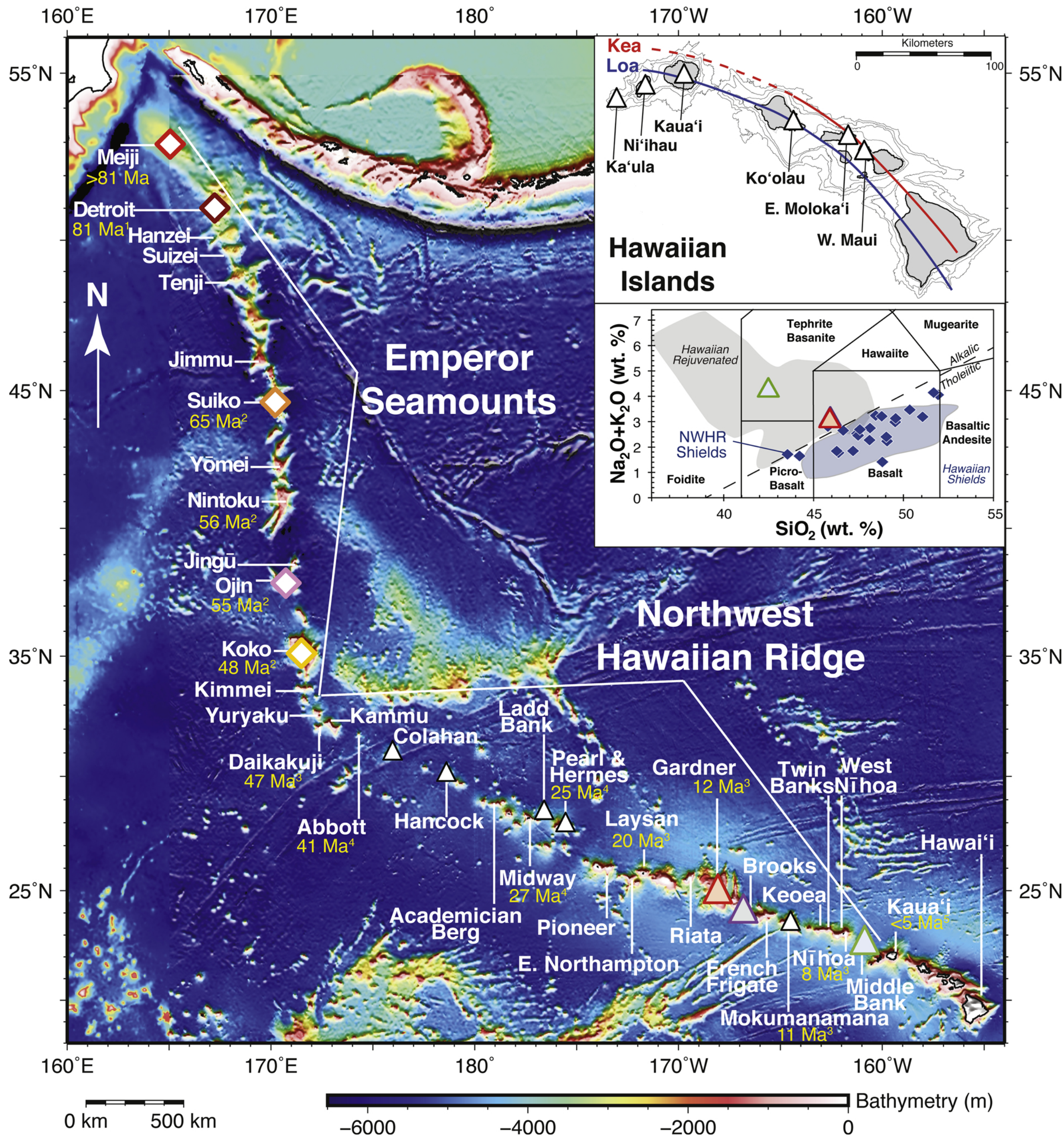

Fig. 1. Bathymetric map of the Hawaiian-Emperor chain.
Bathymetry is 2-minute Gridded Global Relief Data ETOPO2v2 satellite altimetry dataset (U.S. Department of Commerce, National Oceanic and Atmospheric Administration, National Geophysical Data Center, 2006; downloaded March 2014) and new multibeam bathymetry for the NWHR (Smith et al., 2014). Triangles show the location of rejuvenated basalts analyzed in this study. Diamonds show the locations of literature Emperor Seamount data. References for ages are as follows: 1 – Keller et al., 1995; 2 – Clague and Dalrymple, 1987; 3 – Jicha et al., 2018 4 – O'Connor et al., 2013; 5 – Garcia et al., 2010. The Emperor Seamounts stretch from Meiji to Kimmei; the Northwest Hawaiian Ridge from Yuryaku to Middle Bank; and the Hawaiian Islands from Ka'ula to Lō'ihi. Inset figure is a simplified topographic map of the Hawaiian Islands modified from the Main Hawaiian Islands Chart 750-001 Version 17 downloaded from the Hawai'i Mapping Research Group at the University of Hawai'i at Mānoa's website (Main Hawaiian Islands Multibeam Bathymetry Synthesis: www.soest.hawaii.edu) with the Loa and Kea trends shown by blue and red lines, respectively. White triangles show the locations of rejuvenated volcanism on the Hawaiian Islands and includes Ka'ula, Ni'ihau, Kaua'i, O'ahu, East Moloka'i, and West Maui. The other inset figure is a total alkali versus silica plot of NWHR rejuvenated basalts. NWHR rejuvenated samples are all alkalic basalt aside from Middle Bank, which is a tephrite basanite. The tholeiitic-alkalic divide line is from Macdonald and Katsura (1964). NWHR shield data is from Harrison et al. (2017) and Harrison and Weis (2018). The fields for Hawaiian rejuvenated (grey field) and shield-stage (blue field) basalts are shown for comparison. References for the Hawaiian shields are the same as in Harrison and Weis (2018) and are listed in the supplementary information. References for Hawaiian Island rejuvenated data are from Frey et al., 1994, 2005; Roden et al., 1994; Lassiter et al., 2000; Tagami et al., 2003; Yang et al., 2003; Fekiacova et al., 2007; Dixon et al., 2008; Garcia et al., 2010, 2016; Cousens and Clague, 2015; Clague et al., 2016; and Béguelin et al., 2019.

(large low-shear velocity provinces, LLSVP; Garnero et al., 2016 and references therein; Jones et al., 2019; Thomson et al., 2019). Long-lived, deep mantle plumes provide the opportunity to study the geochemical evolution of Earth's reservoirs over time, as well as the dynamics of the sampling of lower mantle material and its transfer to the surface (e.g., White, 2015a, 2015b). Globally, long-lived mantle plumes are rare. In the Indian Ocean, Kerguelen is the longest lived at 100–130 Ma (Coffin et al., 2002); in the Pacific Ocean, the Hawaiian-Emperor (> 81 Ma), Louisville (78 Ma; Koppers et al., 2004), and Rurutu (~120; Koppers et al., 2003) hotspot chains have the longest geologic records (Konrad et al., 2018); and the oldest in the Atlantic Ocean is Tristan da Cunha (132 Ma; Hoernle et al., 2015). The study of long-lived mantle plumes, even if rare, is useful to assess lower-mantle geochemical heterogeneity because of their potential to sample multiple geochemical domains over time (Steinberger, 2000; Steinberger et al., 2004; Boschi et al., 2007; Davies and Davies, 2009; Hassan et al., 2016; Harrison et al., 2017; Bono et al., 2019). The Hawaiian mantle plume is ideally suited for this purpose because it was not involved in continental breakup (which may overwhelm the mantle geochemical signal), has a deep source (French and Romanowicz, 2015), is the oceanic island where the succession of volcanic stages was first noticed and defined (Stearns, 1946), and has been shown to drift in the lower mantle (Steinberger, 2000; Steinberger et al., 2004; Hassan et al., 2015; Harrison et al., 2017). Hawai'i, the archetype of intraplate volcanism, is both the location where hotspot volcanism was first attributed to a mantle plume while paradoxically also displaying a series of unique characteristics not present in any other mantle plume systems in the world. It has among the highest mantle potential temperatures observed in oceanic volcanism and the highest magmatic flux observed in global OIBs (Courtillot et al., 2003; Putirka, 2005). In contrast to other oceanic islands, there is a compositional difference between the shield stage (tholeiitic on Hawai'i) to the other volcanic stages (which are alkalic; Haase et al., 2019), and the magmatic flux appears to be strengthening over time, which is opposite to mantle plume models that predicts a voluminous plume head followed by a weakening plume tail (White, 1993; Jellinek and Manga, 2004; Van Ark and Lin, 2004; Vidal and Bonneville, 2004; Wessel, 2016). Hawai'i therefore represents the end-member of strong-type of mantle plumes, which makes it a key system to study for the understanding of global intraplate volcanism.

Previous studies have focused mainly on the enriched components of deep mantle reservoirs and their potential sources (Frey et al., 1994; Huang et al., 2005b; Huang and Frey, 2005; Sobolev et al., 2005; Jackson et al., 2012; Ballmer et al., 2011; Pietruszka et al., 2013; Frey et al., 2016). The nature, evolution, and potential mantle repositories of Hawaiian depleted components, defined here as material with low time-integrated Rb/Sr (low $^{87}Sr/^{86}Sr$) and high time-integrated Sm/Nd and Lu/Hf ratios (high $^{143}Nd/^{144}Nd$ and $^{176}Hf/^{177}Hf$) relative to primitive mantle, requires a thorough reassessment in light of new observations of mantle dynamics and heterogeneity, and the occurrence of highly depleted compositions in a variety of tectonic environments (Malaviarachchi et al., 2008; Salters et al., 2011; Stracke et al., 2011; Byerly and Lassiter, 2014; Warren, 2016; Genske et al., 2019; 9; Stracke et al., 2019). Here we examine the role of depleted components in Hawaiian-Emperor Chain volcanism and their potential connection to the deep Hawaiian mantle source using data from the oldest rejuvenated basalts analyzed for high-precision isotope ratio and an exhaustive dataset of compiled and renormalized isotope data from the entire Hawaiian-Emperor chain.

1.1. Hawaiian-Emperor chain geology

The Hawaiian-Emperor chain can be divided into three sections (Fig. 1). The oldest section is the Emperor Seamounts (> 81-47 Ma) stretching from the northwestern Pacific Ocean near the Aleutian Islands to the bend in the Hawaiian-Emperor chain (Jackson et al., 1972; Regelous et al., 2003). Next youngest is the Northwest Hawaiian Ridge (NWHR), which is composed of 51 volcanoes spanning ~42 million years and ~2800 km between the bend in the Hawaiian-Emperor chain and the Hawaiian Islands (Sharp and Clague, 2006a, 2006b; Garcia et al., 2015). The youngest section is the Hawaiian Islands, spanning from ~6.5 Ma at Ka'ula to currently active volcanism at Kīlauea and Lō'ihi volcanoes (Sherrod et al., 2007). Hawaiian volcanoes have life-spans characterized by four volcanic stages: 1) alkalic preshield-stage; 2) tholeiitic shield-stage that builds 80–95% of the volcano volume; 3) postshield-stage of mixed alkalic and tholeiitic basalts and 4) rejuvenated-stage of highly alkalic and frequently silica-undersaturated basalts erupted either right after the postshield-stage or after a period of quiescence of up to ~2 Myr (Clague and Dalrymple, 1987; Sherrod et al., 2007; Garcia et al., 2010, 2016; Clague and Sherrod, 2014). Each of these volcanic stages is characterized by different erupted volumes, compositions, geochemical signatures, shallow magmatic processes, xenolith cargos, and mantle sources and do not necessarily occur on all Hawaiian volcanoes (e.g., Feigenson et al., 1983; Frey et al., 1990; Ribe and Christensen, 1999; Xu et al., 2005; Sherrod et al., 2007; Garcia et al., 2010; Hanano et al., 2010; Hofmann and Farnetani, 2013; Clague and Sherrod, 2014; Cousens and Clague, 2015). Shield basalts show the largest range of isotopic variation observed on the Hawaiian Islands, whereas postshield basalts are consistently more isotopically depleted than the shield stage (Hanano et al., 2010; Weis et al., 2011). Rejuvenated-stage basalts present both the most depleted isotopic compositions, defined by high Nd and Hf coupled with low Sr isotopic ratios, and the most limited range in isotopic composition (Lassiter et al., 2000; Frey et al., 2005; Fekiacova et al., 2007; Dixon et al., 2008; Garcia et al., 2010, 2016; Bizimis et al., 2013; Hofmann and Farnetani, 2013; Cousens and Clague, 2015; Béguelin et al., 2019).

1.2. Hawaiian-Emperor chain geochemistry

Recent high-precision isotopic and trace element analyses of NWHR shield-stage basalts fills a gap in the geochemical record for the entire > 81 million year history of the Hawaiian mantle plume (Harrison et al., 2017; Harrison and Weis, 2018), connecting literature studies on the Emperor Seamounts with those from the intensely studied Hawaiian Islands (Keller et al., 2000; Regelous et al., 2003; Frey et al., 2005; Huang et al., 2005a; Sherrod et al., 2007; Tanaka et al., 2008; Weis et al., 2011). Hawaiian Island volcanoes delineate into two geochemical groups, termed the Loa and Kea trends, that also are geographically ordered (i.e., in the Hawaiian Islands, Loa volcanoes are generally the southwest side of the chain whereas Kea volcanoes are generally northeast; Tatsumoto, 1978; Jackson et al., 1972; Abouchami et al., 2005; Huang et al., 2011; Weis et al., 2011; Williamson et al., 2019). The Kea component is present along the entire chain and has been interpreted to originate from the ambient deep Pacific mantle because of its PREMA-like composition (PREMA = PREvalent MAntle, a common composition of all OIB and MORB in multi-isotope space; Zindler and Hart, 1986; Nobre Silva et al., 2013a). The Loa component is more enriched than the Kea component (higher Th/U and Sr isotope ratios with lower Nd and Hf isotope ratios), and is only observed towards the younger end of the Hawaiian-Emperor chain (the oldest sampled volcano to erupt Loa compositions is Daikakuji, dated to ~47 Ma; O'Connor et al., 2013). The origin of the depleted component in Hawaiian basalts is more contentious. On the basis of the geochemical characteristics and longevity of the depleted component, authors have argued for the source to be intrinsic to the plume (Regelous et al., 2003; Bizimis et al., 2005, 2007, 2013; Frey et al., 2005; Huang et al., 2005a; DeFelice et al., 2019), entrained by the plume (Farnetani and Richards, 1995; Keller et al., 2000; Lassiter et al., 2000; Hofmann and Farnetani, 2013), or originating from melting the Pacific lithosphere or asthenosphere (Clague and Dalrymple, 1987; Reiners and Nelson, 1998; Frey et al., 2000; Yang et al., 2003; Béguelin et al., 2019). The hypothesis that the depleted component originates from the upper mantle relies on the observation that it is the dominant component in shield basalts only during the eruption of the oldest Emperor Seamounts (> 70 Ma), when the Hawaiian plume was close to a mid-ocean ridge system (Keller et al., 2000; Regelous et al., 2003). Conversely, other researchers have argued that the geochemical similarity of the depleted component erupted at Detroit Seamount to that in rejuvenated-stage basalts from the Hawaiian Islands suggests it is intrinsic to the plume and present for the entire > 81 million year lifetime of the Hawaiian-Emperor chain (Frey et al., 2005; Huang et al., 2005a; DeFelice et al., 2019). High-precision Pb-Hf-Nd-Sr isotope compositions and trace element concentrations of three available NWHR rejuvenated basalts allow for testing whether the depleted component is present during this ~43 Myr segment of Hawaiian plume activity, and whether or not Hawaiian depleted components erupted at different times have the same composition and potential origin. The compositions of these samples are compared to those of all published Hawaiian rejuvenated basalts and Emperor Seamount shield basalts, a recent compilation of East Pacific Rise MORB data, and Cretaceous and Mesozoic MORB compositions to elucidate the potential relationship between all of these depleted components. Two questions are addressed below: 1. Is the depleted component in Hawaiian basalts the same for the entire > 81 million year history of the Hawaiian-Emperor chain? 2. Is the source of the depleted component in NWHR rejuvenated basalts similar to that contributing to MORB magmatism or does it originate from the lower mantle?

NWHR rejuvenated basalts are distinctive from Cretaceous Emperor Seamount basalts in trace element concentrations and isotope compositions, strong evidence for the presence of separate and different depleted sources for these two groups. The highly depleted source of the Cretaceous Emperor Seamounts is likely a result of interaction of the plume with the Kula-Pacific-Izanagi mid-ocean ridge spreading system. Rejuvenated basalts from the NWHR have among the highest Hf isotope ratios observed from the Hawaiian-Emperor chain and support the existence of a rejuvenated component with limited isotopic variability for at least ~13 Myr. The change in the depleted component from the oldest to the younger Hawaiian-Emperor chain is related to changes in the mechanism of sampling depleted components during the lifetime of the Hawaiian mantle plume. This is essentially different from the processes that govern changes in enriched mantle components during the lifetime of the plume (i.e., by the plume sampling different lower mantle compositional domains throughout time; Weis et al., 2011; Huang et al., 2011; Hoernle et al., 2015; Harrison et al., 2017). Finally, the mechanisms of sampling depleted component(s) and of generating the isotopic composition of erupted rejuvenated lavas are compared between Hawai‘i and other oceanic island alkalic basalts.

2. Temporal and spatial extent of rejuvenated basalts along the Hawaiian-Emperor chain

On the Hawaiian Islands, rejuvenated basalts have been observed on the older third of emergent volcanoes: Ka‘ula, Ni‘ihau, Kaua‘i, Ko‘olau, East Moloka‘i, and West Maui (Clague and Sherrod, 2014). Rejuvenated basalts were previously identified on five NWHR volcanoes: Colahan, Hancock, Ladd Bank, Pearl and Hermes Reef, and Mokumanamana, representing only a very small percentage of total NWHR samples (Clague et al., 1975; Clague and Dalrymple, 1987; Garcia et al., 2015). The rejuvenated stage of NWHR volcanoes was identified based on strongly alkaline composition (e.g., nephelinites or melilitites), elemental characteristics such as low K/Ba and high P_2O_5/Zr, groundmass high-Ca clinopyroxene, and high concentrations of Na, Ti, Al and Ca (Clague et al., 1975; Clague and Dalrymple, 1987; Garcia et al., 2015). Many of these elements are susceptible to mobility by secondary alteration and high-precision isotopic analyses on acid-treated samples are necessary to classify the volcanic stage of samples (e.g., Nobre Silva et al., 2009).

The occurrence of rejuvenated volcanism on some of the oldest Emperor Seamounts (e.g., Detroit, Sueizi, and Teniji guyots) is suggested by the presence of well preserved, sediment-free satellite cones on tilted wave-eroded summit platforms and by the alkalic, xenolith-bearing composition of rocks dredged from some of these cones (Lonsdale et al., 1993). Some of these basalts are silica-undersaturated nepheline melilite, a composition only observed during the rejuvenated-stage, and have concentrations of immobile elements Nb, Ti, and Zr that are typical of very low degrees of partial melting, even lower than observed in Hawaiian Island rejuvenated basalts (Lonsdale et al., 1993). However, the highly evolved alkalic compositions of some cones such as those on Tenji Seamount are more consistent with those of the postshield-stage. Furthermore, the ~20-30 million year hiatus between shield-stage volcanism and cone formation, in addition to the location of cones along faults on Detroit Seamount, may indicate that the cones are associated with tectonic uplift and decompression as the Hawaiian chain collided into the Aleutian, Kamtchaka, and Komondorsky trenches at ~52 Ma rather than being related to the Hawaiian mantle plume (Lonsdale et al., 1993; Kerr et al., 2005). This non plume-related origin is supported by ages of ash layers in the ~800-900 m thick accumulation of sediment on top of Detroit Seamount that post-date the end of shield building by 24–42 million years, much too long to be plume-related rejuvenated-stage (Kerr et al., 2005). Rejuvenated samples were not observed in the studies of Frey et al. (2005) and Huang et al. (2005a) on Detroit Seamount, or in studies on any of the younger Emperor Seamounts (Clague and Dalrymple, 1987; Keller et al., 2000; Regelous et al., 2003; Shafer et al., 2005).

The paucity of rejuvenated-stage basalts along the Emperor Seamounts and the NWHR could be the result of either a sampling bias or a genuine lack of rejuvenated-stage volcanism. Even on the Hawaiian Islands, the rejuvenated-stage of Hawaiian volcanics accounts for less than one percent of shield volcano volume, rejuvenated lavas do not occur on every volcano, and on two shield volcanoes the rejuvenated-stage consists of only a few small cones (Clague and Dalrymple, 1987). Conversely, erosion or sedimentation on the older NWHR and Emperor Seamounts may have removed or buried rejuvenated rocks, compounded by the fact that the small cones that typify the rejuvenated-stage are usually avoided in favor of sample shield-stage volcanic basement in drilling and dredging expeditions.

3. Geological setting and sample locations

The NWHR is comprised of 51 volcanoes and spans ~2800 km (Garcia et al., 2015). Fig. 1 indicates sample locations of the rejuvenated basalts analyzed in this study; XRF major and trace element analyses of some of these samples are reported in Garcia et al. (2015) and Tree (2016) and a detailed description of NWHR sample collection expeditions is given in Harrison et al. (2017). The rejuvenated basalts analyzed in this study were sampled before the Papahānaumokuākea Marine National Monument, a ~1,508,870 km^2 U.S. Marine Conservation Area and World Heritage Site that stretches from Middle Bank to Academician Berg (~80% of the NWHR), was created in 2007. Briefly, multiple expeditions by the Hawai‘i Institute of Geophysics sampled the NWHR from 1972-1984. Although targeting the rejuvenated volcanic stage was not the primary goal of these expeditions, the dredge sampling approach recovered rejuvenated samples at Gardner and Brooks Bank. Both of these samples are weakly olivine phyric (3–5 volume percent olivine) in a matrix with plagioclase, magnetite, and clinopyroxene. Vesicularity is around 10 vol percent with clay in the vesicles and some iddingsite rims on the olivine. Middle Bank was sampled during a 2007 survey of the Northern Hawaiian Islands using the remotely operated vehicle (ROV) *JASON* (Garcia et al., 2008). Two dives recovered 13 samples from the submarine flanks of Middle Bank volcano that mostly belong to the postshield-stage. Dive 303 sampled a rejuvenated cone located on the eastern rift of Middle Bank, and that sample is included here (Garcia et al., 2008).

Classifying the dredged samples from the NWHR into a volcanic stage is complicated by the absence of information on the geological

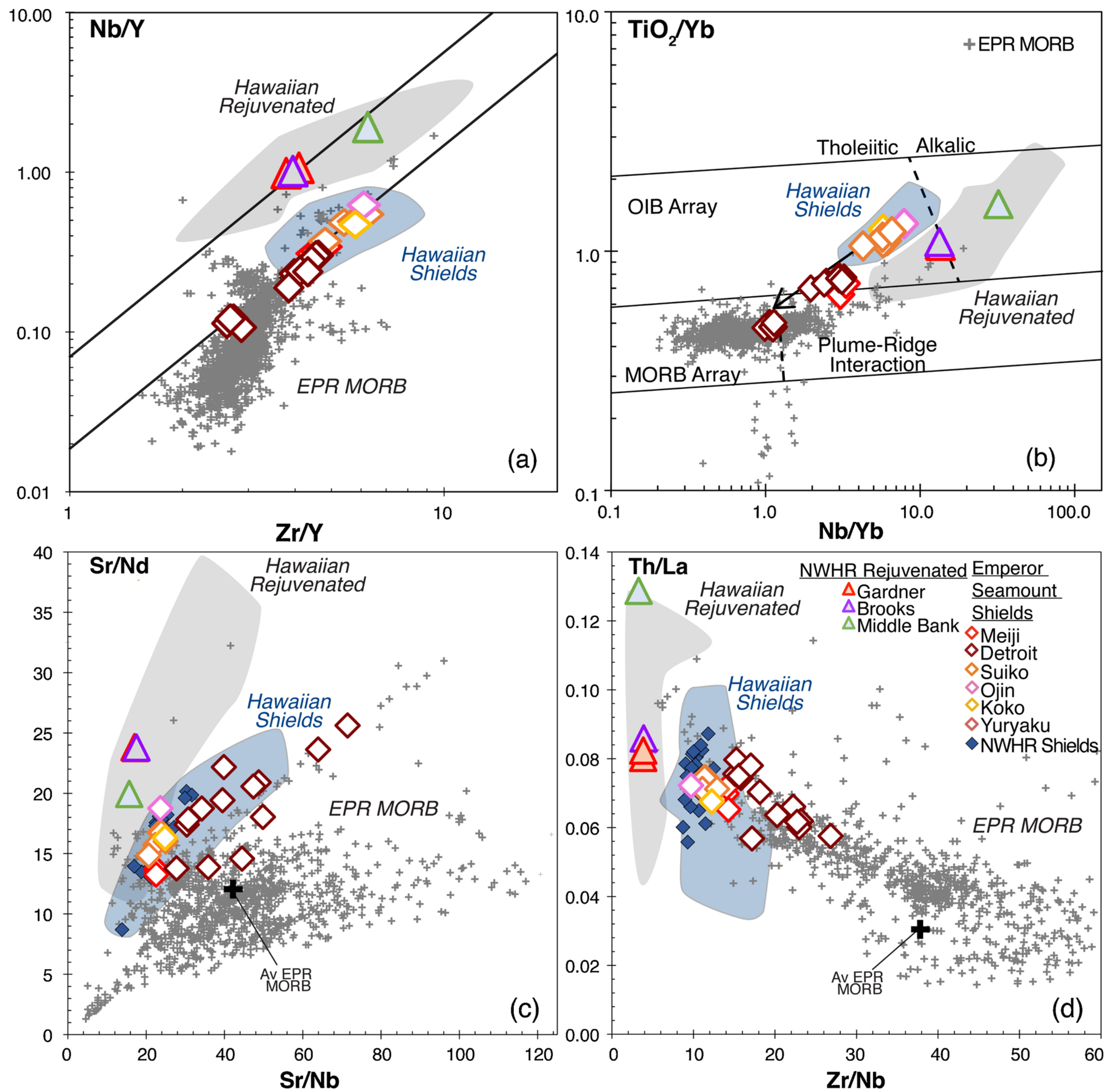

Fig. 2. Trace element plots for classifying volcanic stage and mantle source.
(a) Nb/Y versus Zr/Y, of NWHR shield and rejuvenated basalts following Fitton et al. (1997). (b) TiO_2/Yb versus Nb/Yb of NWHR rejuvenated basalts (diagram from Pearce, 2008). (c) Sr/Nd versus Sr/Nb and (d) Th/La versus Zr/Nb. NWHR rejuvenated basalts plot within the field defined by Hawaiian Island rejuvenated basalts in all of these plots. Sr/Nb and Zr/Nb are insensitive to fractional crystallization processes and show more variation than can be explained by differing degrees of partial melting. Emperor Seamount data defines trends from the fields for the Hawaiian Island shield basalts to that of EPR MORB, a result of interaction with the Kula-Pacific-Izanagi mid-ocean ridge active from > 81-75 Ma. The fields and data sources for the Hawaiian Island shield and rejuvenated basalts are the same as in Fig. 1 and East Pacific Rise (EPR) mid-ocean ridge data was downloaded from the Petrological Database website (www.earthchem.org/petdb) on February 21, 2017; data from Mallick et al., 2019 has been added to this dataset. Emperor Seamount data is from Lanphere et al., 1980; Keller et al., 2000; Regelous et al., 2003; Frey et al., 2005; Huang et al., 2005a.

field relationships (Lonsdale et al., 1993; Garcia et al., 2015). Alteration may undermine the total-alkali versus silica (TAS) rock classification by addition of sodium and removal of potassium and silica, erroneously moving tholeiitic basalts into the alkalic field (Hart et al., 1974; Humphris and Thompson, 1978; Garcia et al., 2015). In this study, volcanic stage classification is guided by the TAS rock classification (Fig. 1 inset) and is confirmed with sample distribution relative to defined fields from Hawaiian Island samples on a Zr/Y versus Nb/Y plot, which is less affected by alteration (Fig. 2a) (Fitton et al., 1997; Greene et al., 2010; Garcia et al., 2015), degree of enrichment in trace elements, and isotopic signature as Hawaiian rejuvenated rocks are characterized by depleted isotopic characteristics: low $^{87}Sr/^{86}Sr$ and high $^{143}Nd/^{144}Nd$ (Tagami et al., 2003; Frey et al., 2005; Xu et al., 2005, 2007; Fekiacova et al., 2007; Garcia et al., 2010, 2016; Bizimis et al., 2013; Cousens and Clague, 2015). Ages of these samples fall along the linear Hawaiian volcanic age progression array, signifying they are consistent with a Hawaiian-plume related source rather than unrelated tectonism which would likely not fall along this line (Jicha et al., 2018). A geologically supported classification requires better sample resolution with high-resolution geochronology on each NWHR volcano, both of which are impossible within the constraints of the current sample collection and the existence of the Papahānaumokuākea Marine National Monument.

Table 1
Pb-Hf-Nd-Sr Isotopic Compositions and Trace Element Concentrations of NWHR Rejuvenated Basalts.

Volcano		Gardner		Gardner		Brooks		Middle Bank	
Sample		72-37C		72-37Cdup		72-41B		301-02	
Distance from Kīlauea (km)		1449		1449		1302		702	
Age (Ma)[ref]		12.46[a]		12.46[a]		12.86[b]		6.5[c]	
Collection Method (year)[ref]		dredge (1976)[1]		dredge (1976)[1]		dredge (1972)[1]		submersible (2007)[2]	
Longitude (°W)		192.1		192.1		193.4		160.6	
Latitude (°N)		25.2		25.2		24.1		22.6	
Trace Element concentration (in ppm)[3]	Sc	27.4		28.3		27.0		24.0	
	V	231		236		226		326	
	Cr	605		589		571		599	
	Co	54.8		53.5		54.5		71.0	
	Ni	193		175		200		384	
	Zn	68		73		73		125	
	Ga	16		16		16		17	
	Cs	0.279		0.284		0.267		–	
	Rb	9.3		10.0		9.7		26.6	
	Sr	499		518		500		772	
	Ba	313		324		294		620	
	Y	27.62		30.59		28.14		25.75	
	Zr	113		116		111		161	
	Hf	3.03		3.00		2.87		3.75	
	Nb	29.35		30.05		28.52		49.20	
	Ta	1.46		1.53		1.44		3.26	
	W	0.65		0.25		1.07		–	
	Li	17.55		18.54		15.02		–	
	La	16.80		16.94		16.77		41.71	
	Ce	36.56		37.97		37.34		78.97	
	Pr	4.70		4.85		4.69		10.44	
	Nd	20.97		21.82		21.02		38.73	
	Sm	5.14		5.34		5.20		8.58	
	Eu	1.81		1.90		1.83		2.63	
	Gd	5.49		5.96		5.57		7.80	
	Tb	0.91		0.94		0.88		1.07	
	Dy	5.18		5.29		5.04		5.61	
	Ho	0.96		0.98		0.95		0.92	
	Er	2.62		2.80		2.56		2.20	
	Tm	0.38		0.36		0.37		0.27	
	Yb	2.20		2.23		2.16		1.55	
	Lu	0.315		0.352		0.301		0.204	
	Pb	1.22		1.18		1.32		2.96	
	Th	1.35		1.39		1.44		5.37	
	U	0.496		0.490		0.452		1.481	
	Isotope Ratios[4]		2SE		2SE		2SE		2SE
Measured Ratios[5]	$^{208}Pb/^{204}Pb$	37.8210	21	37.8309	21	37.8820	147	37.7912	25
	$^{207}Pb/^{204}Pb$	15.4540	8	15.4521	8	15.4766	6	15.4461	8
	$^{206}Pb/^{204}Pb$	18.1975	8	18.2058	8	18.2211	71	18.1487	10
	Th/U[c]	2.27		2.28		0.26		1.82	
U and Age-Corrected Ratios[5]	$^{208}Pb/^{204}Pb_i$	37.777		37.784		37.837		37.759	
	$^{207}Pb/^{204}Pb_i$	15.452		15.450		15.475		15.445	
	$^{206}Pb/^{204}Pb_i$	18.164		18.170		18.187		18.124	
	$^{87}Sr/^{86}Sr_m$	0.703304	10	0.703289	8	0.703293	8	0.703031	9
	$^{87}Sr/^{86}Sr_i$	0.70329		0.70328		0.70328		0.70302	
	$^{143}Nd/^{144}Nd_m$	0.513069	5	0.513050	8	0.513049	6	0.513083	8
	$^{143}Nd/^{144}Nd_i$	0.51306		0.51304		0.51304		0.51308	
	ε_{Nd}[6]	8.5		8.1		8.1		8.7	
	$^{176}Hf/^{177}Hf_m$	0.283202	7	0.283199	5	0.283197	4	0.283105	6
	$^{176}Hf/^{177}Hf_i$	0.28320		0.28320		0.28319		0.28310	
	ε_{Hf}[6]	15.4		15.2		15.2		11.8	

[a]References for ages: a – Jicha et al., 2018; b – Brian Jicha, personal communication; c – Age inferred by interpolating between existing ages and assuming a linear age progression of NWHR volcanoes.
[1,2]Collection method references: 1 - Garcia et al., 1987; 2 - Garcia et al., 2008.
[3]Trace element concentrations (in ppm) were measured on unleached whole rock powders using a Thermo Finnigan Element2 high resolution ICP-MS at the PCIGR at UBC. USGS Reference Material BCR-2 was used for external calibration and a 1 ppb In spike was used as an internal standard. RSDs are less than 5% for all elements and measured concentrations of USGS Standard BHVO-2 are within 2SD of published values.
[4]Hf, Nd, and Pb isotopes were analyzed on a Nu Plasma II MC-ICP-MS and Sr isotopes were analyzed on a Thermo-Finnigan Triton TIMS at the PCIGR. The 2 SE is the absolute error of the individual sample analysis (internal error) and applies to the last decimal place(s). Duplicate and reference material analyses are given in the supplementary information.

[5]All isotope ratios are age corrected to account for radiogenic decay since the time of eruption. For Pb isotope ratios, the measured Th/U ratio is corrected to a Th/U value of 4 (average Th/U of the mantle, all OIB, and average of Hawaiian Island postshield basalts) based on the assumption of U mobility only. These adjusted U concentrations are then used to age correct measured Pb isotopic ratios, correcting for secondary alteration.
[6]ε_{Nd} and ε_{Hf} are calculated using both sample and CHUR values corrected for the age of eruption, starting with present day values of $^{143}Nd/^{144}Nd = 0.512638$ and $^{176}Hf/^{177}Hf = 0.282772$ for chondritic uniform reservoir.
[m,i]m designates the measured isotope ratio and i designates the age-corrected isotope ratio.

4. Analytical techniques

Pb, Hf, Nd, and Sr isotopic compositions and trace element concentrations of three NWHR rejuvenated-type basalts spanning ~5 million years were analyzed at the Pacific Centre for Isotopic and Geochemical Research (PCIGR) at the University of British Columbia (Table 1). Major elements were analyzed by X-ray fluorescence (XRF) at the University of Massachusetts Amherst according to the procedure outlined in Rhodes and Vollinger (2004) and are reported in Garcia et al. (2015) or Tree (2016). The analytical techniques used in this study follow the procedures in Harrison et al. (2017) and Harrison and Weis (2018), as rejuvenated samples were prepared and analyzed during the same sessions.

Briefly, concentrations of trace elements were measured at the PCIGR using a Thermo Finnigan Element2 high resolution ICP-MS and following the method reported in Fourny et al. (2016). Digestion of powdered samples with no prior leaching was accomplished in a 10:1 HNO_3:HF mixture, followed by a 6 N HCl flux to eliminate insoluble fluorides. Samples were then diluted 5000 times, and analyzed on the Element2 using a 1 ppb In spike as an internal standard and the USGS basaltic standard BCR-2 for external calibration. USGS Reference Material BHVO-2 was analyzed with all samples, and resulting values were within two standard deviations of published values for all elements (Schudel et al., 2015; Fourny et al., 2016). Full procedural duplicates and replicate measurements showed excellent agreement, and most elements were analyzed with one relative standard deviation (RSD) of less than 5%.

Samples for isotopic analysis were sequentially acid-leached prior to digestion to remove secondary phases resulting from alteration and possible contamination during sampling. This is especially important for old basalts that have undergone seawater alteration (Hanano et al., 2009; Nobre Silva et al., 2009, 2013b). Acid leaching consisted of successive additions of ~10 mL 6 N HCl to sample powders, ultrasonication for 20 min, followed by immediate decantation before fine particles settled (Weis et al., 2005; Nobre Silva et al., 2009; Fourny et al., 2016). This step was repeated until the supernatant was clear, typically between 6 and 15 steps, after which the sample was rinsed by two final ultrasonication steps of ultrapure distilled water. Samples were then digested using HF and HNO_3, and were purified for the element of interest on chromatographic ion exchange columns, once for isolating Sr, Nd, and Hf, and twice for Pb isotopes (Weis et al., 2005, 2006, 2007; Nobre Silva et al., 2009).

After purification, Pb, Hf, and Nd isotopes were measured on a Nu Plasma MC-ICP-MS II 214 and samples for Sr isotopes were measured on a Thermo-Finnigan Triton TIMS. A Tl spike was added to monitor instrumental mass fractionation of Pb isotope ratios. Instrumental mass fractionation was corrected on-line using isotope ratios of $^{146}Nd/^{144}Nd = 0.7219$, $^{86}Sr/^{88}Sr = 0.1194$, $^{205}Tl/^{203}Tl = 2.3885$, and $^{179}Hf/^{177}Hf = 0.7325$ for Nd, Sr, Pb, and Hf isotope analyses, respectively. Analyses were then normalized off-line to accepted standard values using the sample-standard bracketing method. External reproducibility is established based on repeated analyses of full procedural duplicates of reference materials and is less than 31 ppm for Nd, 20 ppm for Sr, 162 ppm for Pb, and 40 ppm for Hf (see supplementary information for reference material analyses).

The accuracy of sample analyses was controlled by repeat analyses of international reference materials and standards as well as duplicate and replicate analyses of samples. For the two-year duration of this study the measured isotopic signatures for international isotope standards are as follows: $^{143}Nd/^{144}Nd = 0.512071 \pm 0.000034$ for Nd standard JNdi (2SD, n = 63), $^{176}Hf/^{177}Hf = 0.282164 \pm 0.000031$ for Hf standard JMC 475 (2SD, n = 99), $^{87}Sr/^{86}Sr = 0.710243 \pm 0.000020$ for Sr standard SRM 987 (2SD, n = 19), and $^{208}Pb/^{204}Pb = 36.7188 \pm 0.0107$, $^{207}Pb/^{204}Pb = 15.4983 \pm 0.0041$, and $^{206}Pb/^{204}Pb = 16.9418 \pm 0.0028$ for Pb standard SRM 981 (2SD, n = 102). Repeated analyses of U.S. Geological Survey (USGS) reference material BHVO-2, a Hawaiian basalt, resulted in average isotope compositions of $^{87}Sr/^{86}Sr = 0.703466 \pm 0.000011$ (2SD, n = 3), $^{143}Nd/^{144}Nd = 0.512991 \pm 0.000016$ (2SD, n = 3), $^{176}Hf/^{177}Hf = 0.283103 \pm 0.000001$ (2SD, n = 3), $^{208}Pb/^{204}Pb = 38.2119 \pm 0.0062$, $^{207}Pb/^{204}Pb = 15.4900 \pm 0.0005$, and $^{206}Pb/^{204}Pb = 18.6482 \pm 0.0001$ (2SD, n = 2). These isotope ratios are within the range of published values (Weis et al., 2005, 2006, 2007; Chauvel et al., 2010; Nobre Silva et al., 2013b; Fourny et al., 2016). Epsilon Nd and epsilon Hf are calculated using both sample and CHUR values corrected for the age of eruption, starting with present day values of $^{143}Nd/^{144}Nd = 0.512638$ and $^{176}Hf/^{177}Hf = 0.282772$ for chondritic uniform reservoir (CHUR; Jacobsen and Wasserburg, 1980; Blichert-Toft and Albarède, 1997).

NWHR basalts analyzed in this study were age corrected to account for in situ radiogenic decay since the time of eruption. Sr, Nd, and Hf isotope ratios were age-corrected based on the parent and daughter element concentrations measured in unleached NWHR basalts powders. For age-correction of Pb isotope ratios the method of Nobre Silva et al. (2013b) that corrects potentially altered U concentrations measured in unleached sample powders to canonical ratio values of Th/U was employed (see Harrison et al., 2017 for a detailed discussion of the method). This method corrects altered U concentrations to the average Th/U ratio of Hawaiian shield or postshield and rejuvenated basalts assuming Th is immobile during secondary alteration (Nobre Silva et al., 2013b). A Th/U = 3 [n = 294] was used to correct shield basalts and a Th/U = 4 [n = 217] was used for postshield and rejuvenated basalts (Harrison et al., 2017); both Th/U ratios are very similar to the Th/U ratio of global OIB (O'Nions and McKenzie, 1993). This age correction technique was also applied to literature Emperor Seamount Pb isotope data (Regelous et al., 2003; Frey et al., 2005; Huang et al., 2005a), and provides a better approximation of the erupted U concentrations than in previous studies that used the measured U concentration in leached sample powders, a procedure that tends to leach elements incongruently and results in non-reproducible parent isotope concentrations (Regelous et al., 2003; Huang et al., 2005a; Shafer et al., 2005; Hanano et al., 2009; Nobre Silva et al., 2009). Applying this modified age correction technique has significantly reduced the scatter in Emperor Seamount Pb isotope data, allowing for a finer interpretation of Emperor Seamount mantle sources.

In order to compare new NWHR analyses with existing data, a database of isotopic compositions and trace and major element concentrations was compiled for Hawaiian Island and Emperor Seamount shield and rejuvenated basalts (GeoRoc Geochemical Database: georoc.mpch-mainz.gwdg.de/georoc). EPR MORB data was downloaded from the petrological database of the Ocean Floor (PetDB: http://www.petdb.org) and Pacific Mesozoic and Cretaceous MORB data from Pacific oceanic crust drill cores of the targeted age ranges were compiled from the following sources: Janney and Castillo (1997); Sano and Hayasaka (2004); Brandl et al. (2013), and Heydolph et al. (2014). Oceanic islands with documented occurrences of rejuvenated volcanism were also downloaded and sorted based on volcanic stage. All compiled isotopic data was normalized to the same isotopic standard values to ensure comparability and a coherent dataset (Weis et al., 2011). Nd isotopes are normalized to a $^{143}Nd/^{144}Nd$ La Jolla value of 0.511858; Sr isotopes to a $^{87}Sr/^{86}Sr$ SRM 987 value of 0.710248; Hf to a $^{176}Hf/^{177}Hf$ JMC 475 value of 0.282160; and Pb isotopes to a SRM 981 values of 16.9405 for $^{206}Pb/^{204}Pb$, 15.4963 for $^{207}Pb/^{204}Pb$, and 36.7219 for $^{208}Pb/^{204}Pb$ (Weis et al., 2005, 2006, 2007).

5. Results

5.1. Major and trace elements of NWHR rejuvenated basalts

The composition of rejuvenated basalts from the Northwest Hawaiian Ridge varies from basanite to alkali basalt (Fig. 1 inset). The concentration of MgO is between 10–14 wt%, within the range observed in Hawaiian Island rejuvenated basalts (MgO concentrations 5.6–15 wt%; e.g., Clague and Frey, 1982; Garcia et al., 2016). Samples from Brooks Bank, Gardner, and Middle Bank consistently overlap with Hawaiian Island rejuvenated basalts with low SiO_2 and Zr and high P_2O_5, Nb, Sr, and Ba (Figs. 3, 4). Middle Bank exhibits the greatest enrichments of highly incompatible trace elements and are likely the result of the low degrees of partial melting (Figs. 3, 4).

As observed on the Hawaiian Islands, rejuvenated basalts of the NWHR are more enriched in incompatible trace elements than their corresponding shield-stage (Gardner and Middle Bank are NWHR volcanoes where samples from both the shield and rejuvenated volcanic stages were recovered; Figs. 2–5). The distinctive elemental concentrations of HREE, Hf, Nb, and Sr of the Hawaiian rejuvenated basalts have been interpreted as a result of the presence of residual phlogopite, garnet, and Fe-Ti oxides in the mantle source (Clague and Frey, 1982; Yang et al., 2003; Clague et al., 2016). Highly refractory elements Ti, Zr, Hf, Nb, and Ta are depleted relative to elements of similar incompatibility in many NWHR rejuvenated samples, as has been also observed in the Honolulu Volcanics (Clague and Frey, 1982). Scandium concentrations are high, comparable to Ka'ula rejuvenated basalts, suggesting absent or minor clinopyroxene fractionation in NWHR rejuvenated basalts (Cousens and Clague, 2015; Garcia et al., 2016). NWHR rejuvenated basalts have higher Nb/Y, $(La/Sm)_{PM}$, $(Th/Ce)_{PM}$, and $(La/Yb)_{PM}$ with lower Sr/Nb and Zr/Nb than Hawaiian shield basalts (Figs. 2, 5).

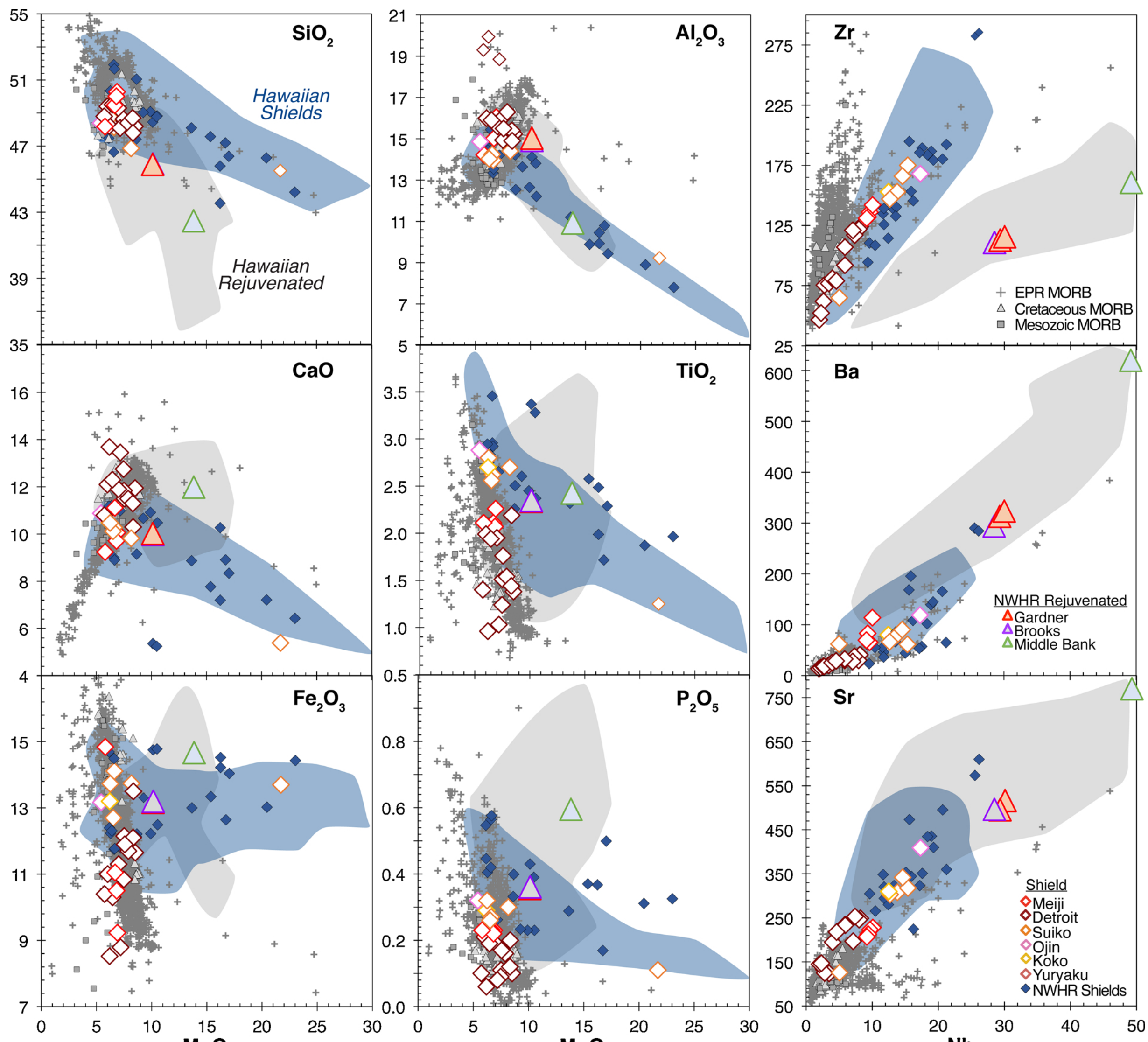

Fig. 3. MgO variation plots of selected NWHR rejuvenated basalt major and minor elements.
The fields and data sources for the Hawaiian Islands are the same as in Fig. 1 and EPR MORB data is the same as in Fig. 2. Mesozoic and Cretaceous MORB data is from Janney and Castillo (1997); Sano and Hayasaka (2004); Brandl et al. (2013), and Heydolph et al. (2014). The field of Hawaiian Island and NWHR rejuvenated basalts is different from Emperor Seamount shield basalts, which illustrates the differences in source between the groups.

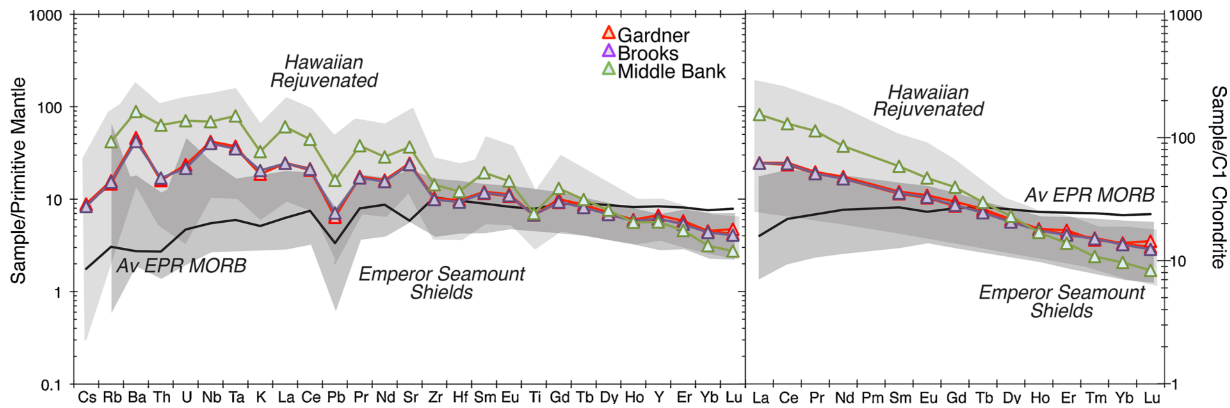

Fig. 4. Primitive mantle-normalized extended trace element and chondrite-normalized rare earth element plots of NWHR rejuvenated basalts.
Primitive mantle and chondrite normalizing values are from McDonough and Sun (1995). Hawaiian Island rejuvenated basalts define the light grey field in the background (data sources are given in Fig. 1) and the dark grey field in the background are Emperor Seamount shield basalts (Regelous et al., 2003; Huang et al., 2005a). The black line is the average of all EPR MORB, downloaded from the Petrological Database website (www.earthchem.org/petdb) on February 21, 2017. Element incompatibility increases towards the left.

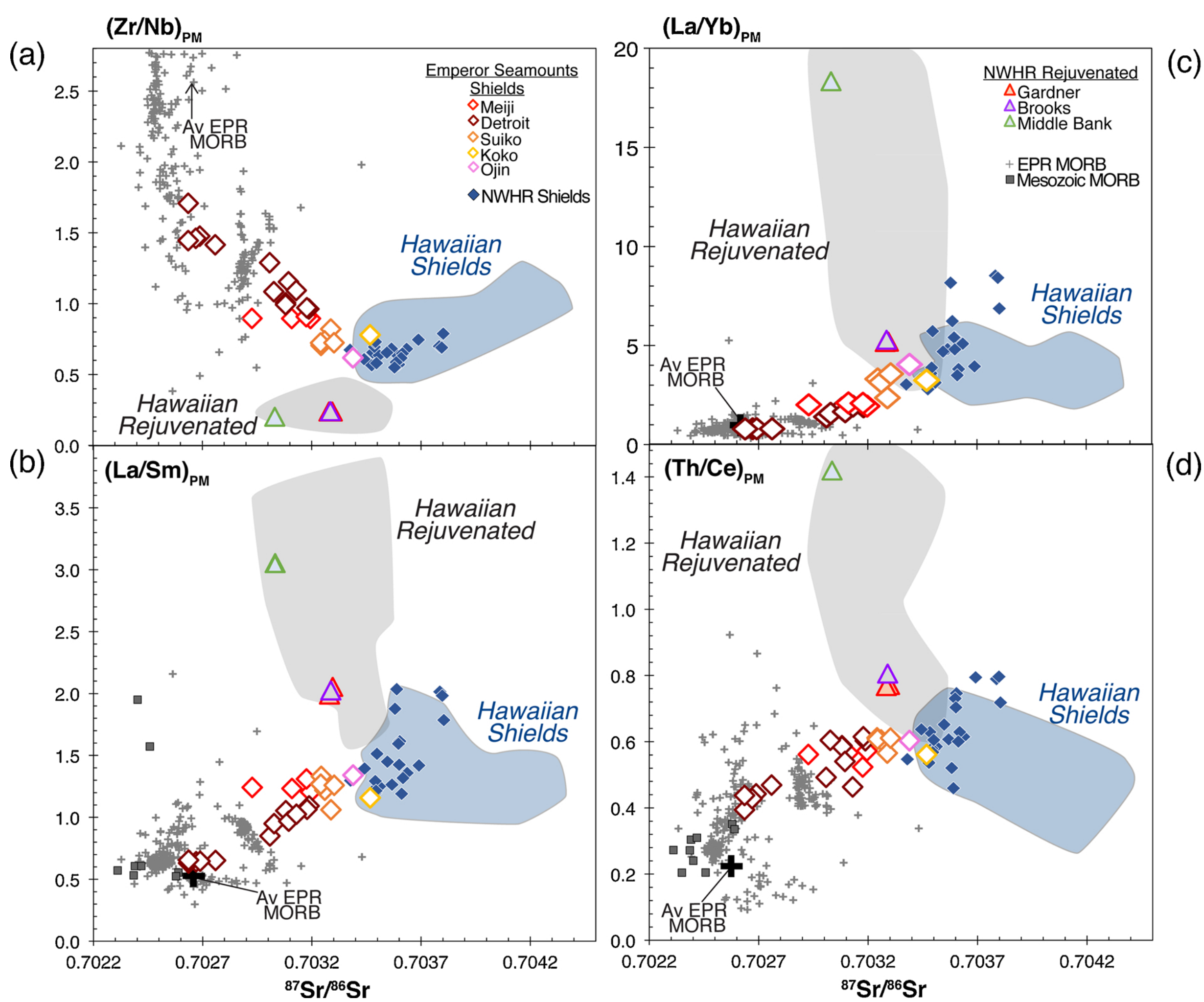

Fig. 5. Trace element ratio variation plots of NWHR rejuvenated basalts.
Primitive mantle-normalized trace element ratios of (a) Zr/Nb, (b) La/Sm, (c) La/Yb, and (d) Th/Ce versus $^{87}Sr/^{86}Sr$. NWHR rejuvenated basalts and the oldest Emperor Seamount shield basalts form arrays in diverging directions from Hawaiian Island shield basalts in plots a-d, indicating different depleted components for each group. The Emperor Seamounts overlap with EPR MORB compositions, and the NWHR rejuvenated basalts trend in the opposite direction from EPR MORB compositions. The fields and data sources for the Hawaiian Islands are the same as in Fig. 1 and EPR MORB and Emperor Seamount data sources are the same as in Fig. 2. Mesozoic MORB data is from Sano and Hayasaka (2004) and Brandl et al. (2013). All Sr isotope ratios are re-normalized to the same standard values.

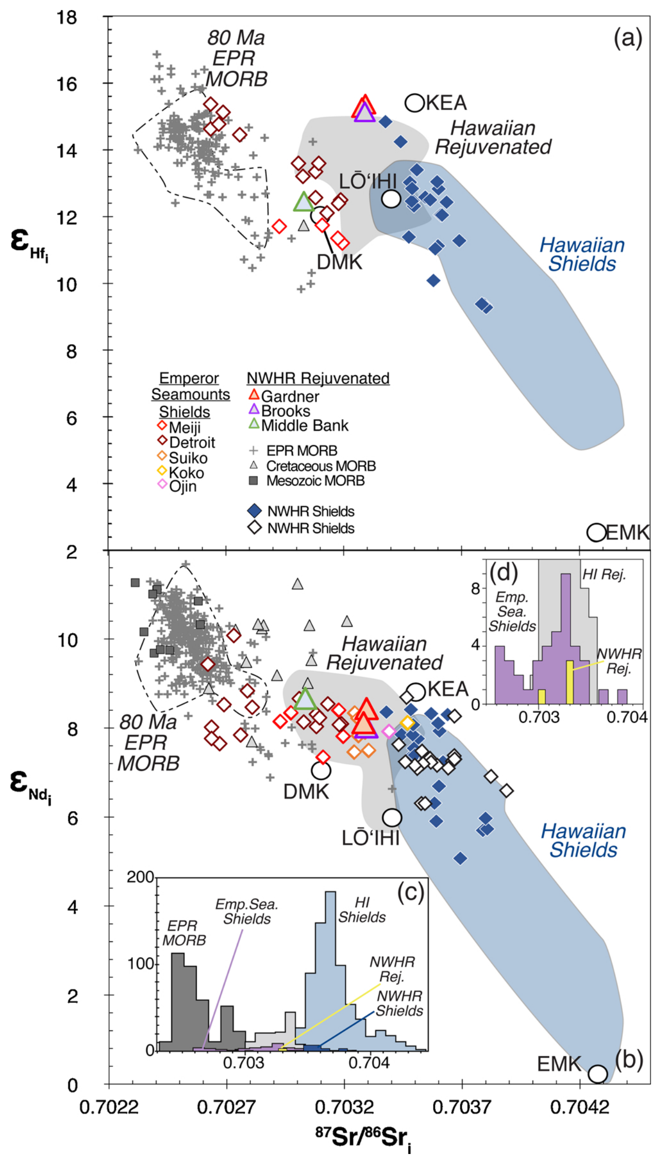

Fig. 6. Nd, Sr, and Hf isotope compositions of NWHR rejuvenated basalts. (a) Epsilon Hf versus $^{87}Sr/^{86}Sr$ (b) Epsilon Nd versus $^{87}Sr/^{86}Sr$. Two SE error bars on new NWHR analyses are smaller than data points. Inset figures (c) shows the $^{87}Sr/^{86}Sr$ of EPR MORB (dark grey field), Emperor Seamount shield basalts (Emp. Sea. Shields, orange field), Hawaiian Island rejuvenated basalts (HI Rej., light grey field), NWHR rejuvenated basalts (NWHR Rej., yellow field), NWHR shield basalts (NWHR shields, dark blue field), and Hawaiian Island shield basalts (HI Shields, light blue field). Inset figure (d) is a zoomed in scale of inset figure (c) showing Emperor Seamount shield basalts, NWHR rejuvenated basalts, and Hawaiian Island rejuvenated basalts only. The fields and data sources for the Hawaiian Islands are the same as in Fig. 1 and EPR MORB and Emperor Seamount data is the same as in Fig. 2; all isotopic data is normalized to the same isotope standard values. In addition to normalized EPR MORB data (grey plus symbols), the field for EPR MORB data age corrected to 80 million years is shown by the dashed black line as an approximation of the same mantle source at the time of the formation of the oldest Emperor Seamounts. For reference the four Hawaiian end-member components are shown by white circles (DMK, EMK, Lōʻihi, Tanaka et al., 2002, 2008; KEA, Harrison and Weis, 2018). Mesozoic and Cretaceous MORB data is normalized to the same isotopic standards and is from Janney and Castillo (1997); Sano and Hayasaka (2004); Brandl et al. (2013), and Heydolph et al. (2014). Blue diamonds show recent leached isotopic analyses of NWHR basalts (Harrison et al., 2017; Harrison and Weis, 2018) while white diamonds with a black outline designate older leached (Regelous et al., 2003) and unleached (Lanphere et al., 1980; Basu and Faggart, 1996) NWHR isotope analyses.

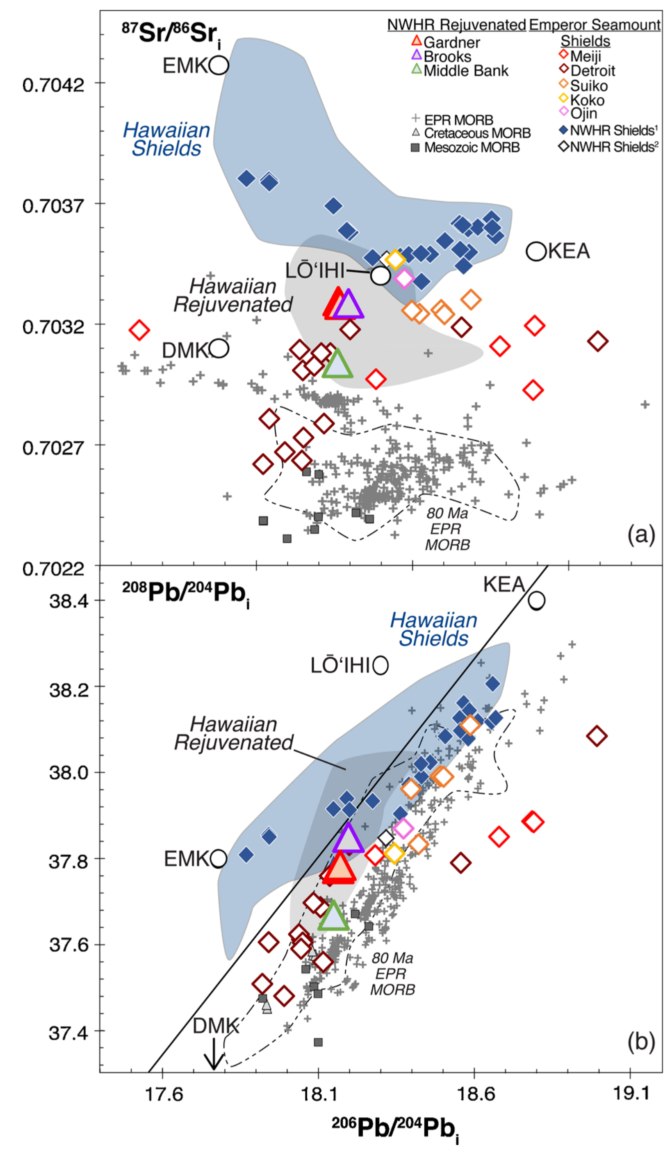

Fig. 7. Pb and Sr isotopic compositions of NWHR rejuvenated basalts. (a) $^{87}Sr/^{86}Sr$ versus $^{206}Pb/^{204}Pb$ (b) $^{208}Pb/^{204}Pb$ versus $^{206}Pb/^{204}Pb$. The black line is the Loa-Kea boundary from Abouchami et al. (2005). Two SE error bars on new NWHR analyses are smaller than data points. Figure data sources and symbols are the same as in Fig. 6; all isotopic data is normalized to the same standard values.

5.2. Pb-Hf-Nd-Sr isotopic compositions of NWHR rejuvenated basalts

New NWHR isotopic data extends the range of Hf isotopic compositions found in Hawaiian rejuvenated basalts to the highest values ever observed (up to 15.4 epsilon Hf at Gardner) (Figs. 6, 8 and 9). High Hf isotopic compositions occur at Gardner and Brooks Bank, two of the locations where magmatic flux is the highest along the NWHR (Van Ark and Lin, 2004; Vidal and Bonneville, 2004; Wessel, 2016). Rejuvenated NWHR basalts overlap in Sr and Nd isotopes with Hawaiian Island rejuvenated basalts (i.e., generally high in $^{143}Nd/^{144}Nd$ and low in $^{87}Sr/^{86}Sr$) (Figs. 6, 8). These basalts also present depleted, Hawaiian Island rejuvenated-like isotopic signatures, with Middle Bank exhibiting the most depleted $^{87}Sr/^{86}Sr$ signatures (~0.70302; Figs. 6, 7). In a $^{208}Pb/^{204}Pb$-$^{206}Pb/^{204}Pb$ isotope plot, rejuvenated basalts all plot on the Kea side of the Abouchami et al. (2005) Loa-Kea divide line in the same field as all Hawaiian Island rejuvenated basalts (Fig. 7b; Frey et al., 1994, 2005; Roden et al., 1994; Lassiter et al., 2000; Tagami

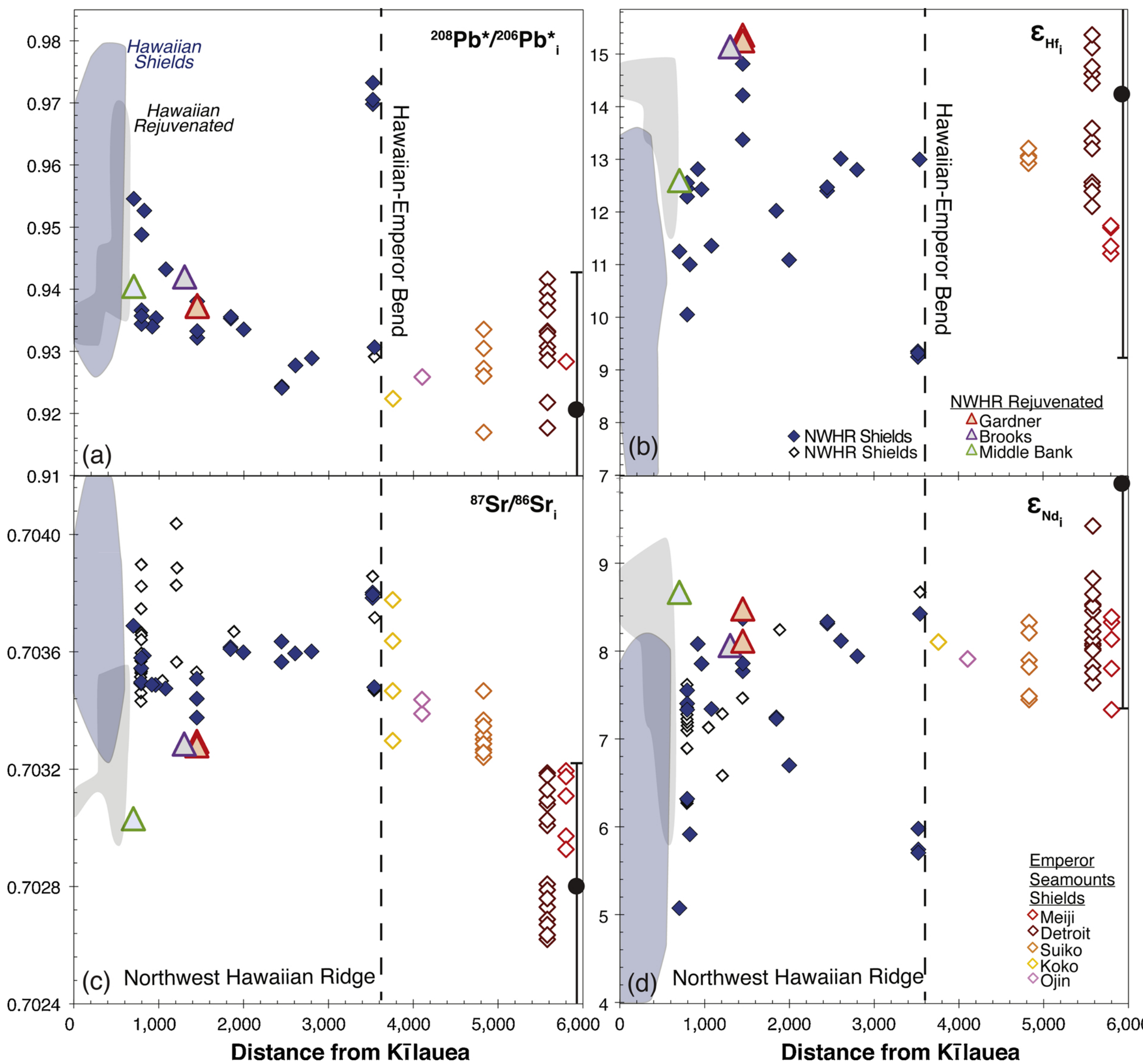

Fig. 8. Isotopes versus distance from Kīlauea for the Hawaiian-Emperor chain.
(a) $^{208}Pb^{*}/^{206}Pb^{*}$ (b) epsilon Hf (c) $^{87}Sr/^{86}Sr$ (d) epsilon Nd versus distance from Kīlauea (a proxy for age). Two SE error bars on new NWHR analyses are smaller than data points. Figure data sources and symbols are the same as in Fig. 6; all isotopic data is normalized to the same standard values. The black circle is the average of EPR MORB with 2 standard deviation error bars.

et al., 2003; Yang et al., 2003; Fekiacova et al., 2007; Dixon et al., 2008; Garcia et al., 2010, 2016; Cousens and Clague, 2015; Clague et al., 2016; Béguelin et al., 2019). The isotopic composition of NWHR rejuvenated basalts is indistinguishable from Hawaiian Island rejuvenated basalts and requires the presence of a rejuvenated component with a consistent composition for at least 12.5 million years.

5.3. The composition of Cretaceous Emperor Seamounts

Geochemically, the older Emperor Seamounts (e.g., Detroit, Meiji, and Suiko, 81-65 Ma) define a continuum between EPR MORB compositions and Hawaiian "plume-signature" composition as defined by the Hawaiian Islands and NWHR shield-stage basalts (Figs. 2, 5–7, 9). The younger Emperor Seamounts (e.g., Ojin and Koko) plot in the field defined by shield-stage basalts from the NWHR and Hawaiian Islands. Strontium isotopic ratios of the Cretaceous Emperor Seamounts are unradiogenic with values that are close to the average of global MORB; values become more radiogenic to the south for the younger Emperor Seamounts (Figs. 6, 7a, 8 c) (Keller et al., 2000; Regelous et al., 2003; Frey et al., 2005; Huang et al., 2005a; Gale et al., 2013). Shield and postshield samples from Meiji and Detroit Seamounts show the most depleted $^{87}Sr/^{86}Sr$ isotopic ratios measured along the Hawaiian-Emperor chain (Regelous et al., 2003; Frey et al., 2005; Huang et al., 2005a). Generally, Emperor Seamount basalts plot between the fields defined by Cenozoic Hawaiian lavas and the NWHR as a group and East Pacific Rise MORB in epsilon Nd, $^{87}Sr/^{86}Sr$, $^{206}Pb/^{204}Pb$, and epsilon Hf (Figs. 6–8). In He isotopic signature, Detroit samples overlap with MORB values (average $^{3}He/^{4}He$ of Detroit = 9.77 ± 1.75 R_A vs. average MORB is 8 ± 1 R_A), whereas the younger Emperor Seamounts, Suiko and Koko, reach much higher, plume-like He isotopic compositions ($^{3}He/^{4}He$ from 18 to 24 R_A; Keller et al., 2004; Broadley et al., 2018). The composition of halogens in Emperor Seamount basalts follows the same trend with Detroit Seamount Br/Cl and I/Cl ratios similar to MORB whereas Suiko and Koko have higher ratios indicative of an addition of altered oceanic crust (Broadley et al., 2018). The MORB-like He isotope ratios and depleted incompatible and halogen element concentrations of the Cretaceous Emperor Seamounts are consistent with a plume-ridge interaction (e.g., White, 2015a, 2015b and references therein).

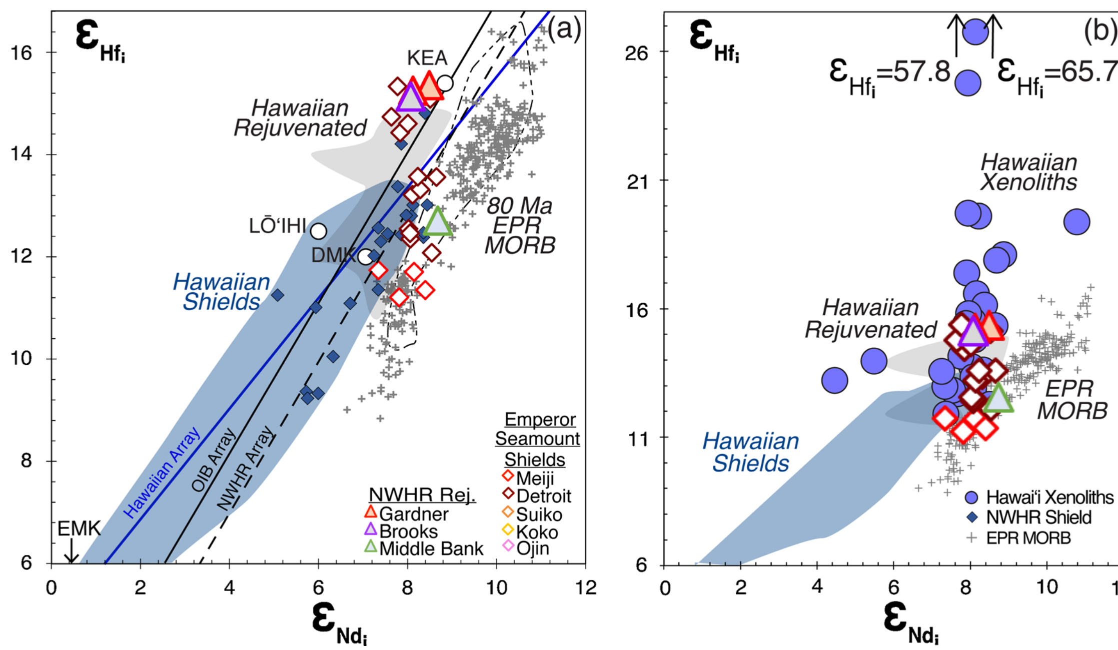

Fig. 9. Nd and Hf isotopic variation of NWHR rejuvenated basalts.
(a) Epsilon Hf versus epsilon Nd. The Hawaiian and NWHR arrays are from Harrison and Weis (2018), and the OIB array is from Blichert-Toft et al. (1999). Two SE error bars on new analyses are smaller than data points. In addition to normalized EPR MORB data (grey plus symbols), the field for EPR MORB data age corrected to 80 million years is shown by the dashed black line as an approximation of the same mantle source at the time of the formation of the oldest Emperor Seamounts. For reference the four Hawaiian end-member components are shown by white circles (DMK, EMK, Lōʻihi, Tanaka et al., 2002, 2008; KEA, Harrison and Weis, 2018). (b) Epsilon Hf versus epsilon Nd of Hawaiian xenoliths, which exhibit very high epsilon Hf values (yellow circles; note the same scale for epsilon Nd as figure a and the expanded scale for epsilon Hf). The blue field is Hawaiian shields and the grey field is Hawaiian rejuvenated basalts. Hawaiian xenolith data is from Frey et al., 2005; Bizimis et al., 2003, 2005, 2007. Figure data sources and symbols are the same as in Fig. 6; all isotopic data is normalized to the same standard values.

6. Discussion

All Emperor Seamount basalts have Kea-like Nd isotopic signature regardless of volcanic stage, and Sr, Pb, and Hf isotopic ratios that are more depleted than those of the Kea component (Keller et al., 2000; Regelous et al., 2003; Frey et al., 2005; Huang et al., 2005a; Shafer et al., 2005; Tanaka et al., 2008). The Loa trend is ephemerally present in shield-stage samples along the NWHR (Harrison et al., 2017; Harrison and Weis, 2018), and a greater volume of shield basalts from the Hawaiian Islands belong to the Loa trend than the Kea trend (Weis et al., 2019). Some Emperor Seamount basalts have anomalously low $^{87}Sr/^{86}Sr$ isotopic ratios, moderate to high $^{143}Nd/^{144}Nd$ isotope ratios, and low abundances of incompatible trace elements relative to shield basalts from the Hawaiian Island (Fig. 4; Keller et al., 2000; Regelous et al., 2003; Frey et al., 2005; Huang et al., 2005a). The distinct isotopic characteristics of the Emperor Seamounts were previously explained by their formation on thinner, younger lithosphere that allowed for greater degrees of melting of a refractory, more depleted plume component (Regelous et al., 2003; Frey et al., 2005; Huang et al., 2005a). The depleted component was proposed to be intrinsic to the plume, and the same as in the source of Hawaiian Island rejuvenated basalts (Frey et al., 2005; Huang et al., 2005a). An alternative explanation for the depleted component in Emperor Seamount basalts was a plume-ridge interaction that resulted in mixing of upper depleted mantle with Hawaiian plume melts (Keller et al., 2000). This interpretation requires the presence of a different depleted component than the one present in the source of Hawaiian rejuvenated basalts. The geochemical signature of depleted sources present in Hawaiian basalts are compared below, with implications for source evolution of the entire Hawaiian-Emperor chain and the origin of Hawaiian rejuvenated basalts.

6.1. NWHR rejuvenated basalts: a homogeneous rejuvenated component over ~12.5 Myr

NWHR rejuvenated basalts define a limited range in isotopic signature relative to the observed range for Hawaiian shield-stage basalts. This composition is present for at least ~12.5 Myr, as it overlaps with those observed in Hawaiian Island rejuvenated basalts which themselves define the most limited range of variation in isotopic signature of any Hawaiian volcanic stage (Clague and Frey, 1982; Garcia et al., 1987; Lassiter et al., 2000; Tagami et al., 2003; Frey et al., 2005; Xu et al., 2005, 2007; Fekiacova et al., 2007; Dixon et al., 2008; Garcia et al., 2010, 2016; Cousens and Clague, 2015; Béguelin et al., 2019). Lavas as old as ~38.7 Ma have been attributed to the rejuvenated stage on the basis of their major and trace element composition (Duncan and Clague, 1984; Sharp and Clague, 2006a, 2006b; Garcia et al., 2015). If these lavas are confirmed to have isotopic signatures consistent with those of younger Hawaiian rejuvenated lavas, the presence of this depleted composition would be extended to almost 40 Ma. The consistency of the rejuvenated basalt composition is notable considering the relative changes in shield-stage compositions over the same time period (Basu and Faggart, 1996; Harrison et al., 2017; Harrison and Weis, 2018). The Loa geochemical composition is observed in shield-stage basalts of the NWHR for the first time at Daikakuji (~47 Ma) and in increasing amounts towards the younger end of the ridge southeast of Midway (Regelous et al., 2003; Harrison et al., 2017; Harrison and Weis, 2018). Regardless of when the Loa geochemical composition arrived along the NWHR during the shield volcanic stage, NWHR rejuvenated volcanism is consistent in isotopic composition, independent of the composition of the shield-stage Loa (e.g., Middle Bank) and Kea (e.g., Gardner, Brooks Bank) volcanoes. This suggests that the source component of these rejuvenated basalts is not directly related to the shield-stage source. Similarly, on the Hawaiian Islands, Loa trend (e.g., Koʻolau, Kauaʻi) and Kea trend (e.g., Niʻihau, East Molokaʻi, West Maui) volcanoes erupt rejuvenated basalt of a consistent composition within the limited range of isotopic composition defined by the rejuvenated volcanic stage relative to other Hawaiian volcanic stages (Frey et al., 1994, 2005; Roden et al., 1994; Lassiter et al., 2000; Tagami et al., 2003; Yang et al., 2003; Fekiacova et al., 2007; Dixon et al., 2008; Garcia et al., 2010, 2016; Cousens and Clague, 2015; and Clague et al., 2016). It is important to note that published literature on the isotopic variation in Hawaiian Island shield-stage basalts has proposed the participation of a depleted component in order to describe the variation observed in Kauaʻi shield basalts (expanded to other Hawaiian volcanoes based on a statistical analysis), Koʻolau shild drillcore samples, and an anomalous 50 m long section of isotopically depleted basalts from Mauna Kea drilled during the Hawaii Scientific Drilling Project (HSDP; Mukhopadhyay et al., 2003; Salters et al., 2006; Tanaka et al., 2008; DeFelice et al., 2019). The shield stage of Hawaiian volcanoes is generated through considerably more melting and record a much larger range of isotopic variation than the rejuvenated stage; it is possible that the depleted component is ubiquitous in the mantle and mostly unobserved due to its refractory nature and dilution by more fusible components (Frey et al., 2005; Malaviarachchi et al., 2008; Salters et al., 2011; Byerly and Lassiter, 2014; Mougel et al., 2014, 2015; Sanfilippo et al., 2019). Nevertheless, rejuvenated basalts represent less than one percent of the volume of a Hawaiian volcano (Clague and Sherrod, 2014) and the consistency of the composition of these lavas at such low amounts of melt generation is surprising given that small degrees of melting are typically associated with sampling more heterogeneity in the Hawaiian mantle plume rather than less (Fig. 10).

6.2. Multiple Hawaiian depleted components

The composition of Hawaiian rejuvenated lavas appears to be relatively isotopically homogeneous during the duration they are observed along the Hawaiian-Emperor chain, but there are other instances when depleted compositions appear in Hawaiian lavas. These potentially different depleted components that participate in Hawaiian volcanism can be distinguished using diagnostic trace element ratios. For example, Sr/Nb and Zr/Nb are insensitive to differentiation processes unless plagioclase is involved (Frey and Rhodes, 1993) and the similar incompatibilities of Sr and Nd imply they will not fractionate significantly during partial melting (Figs. 2, 5). Hawaiian Island and NWHR shield-stage basalts define the field of the Hawaiian plume source in these plots (shown by the blue shaded field) and Hawaiian Island rejuvenated basalts and EPR MORB define the two possible depleted components that may contribute to the source of NWHR rejuvenated basalts. In all of these plots, the oldest Emperor Seamounts (Meiji and Detroit) partly overlap with the EPR MORB field while Hawaiian rejuvenated basalts and NWHR rejuvenated basalts trend in the opposite direction (Figs. 2, 5). The lower Nb and Sr of Emperor Seamount basalts yield higher Zr/Nb and Sr/Nb (Fig. 2), whereas Hawaiian rejuvenated basalts are distinctively low in Zr/Nb and high in LREE, $(Th/Ce)_{PM}$, and $(Zr/Nb)_{PM}$ ratios (Figs. 2, 5).

In Fig. 2b the Hawaiian Islands, NWHR, and Emperor Seamounts define a trend between the fields of EPR MORB and that of Hawaiian shield basalts. This relationship is also observed in other oceanic island settings with documented plume-ridge interactions such as Iceland, the Galápagos, the Red Sea and Red Sea Islands, Kerguelen and the Ninetyeast Ridge, Easter Island and the East Pacific Rise, Bouvet Island and the South America-Antarctic Ridge, Jan Mayen and the Kolbeinsey Ridge, and Tristan-Gough Island and the Mid-Atlantic Ridge (Kingsley and Schilling, 1998; Murton et al., 2002; Pearce, 2008; Harpp et al., 2014). NWHR and Hawaiian rejuvenated basalts, conversely, plot in a separate field (Fig. 2b), indicating both differences in degree of partial melting (TiO_2, Y, and Yb concentrations) and differences in source (Nb and Zr concentrations; Fitton et al., 1997; Pearce, 2008). This suggests that Emperor Seamount and rejuvenated basalts have both different sources and degrees of partial melting.

6.3. The depleted mantle component in Cretaceous Emperor Seamounts

Unradiogenic Pb isotope ratios of Detroit basalts do not overlap with EPR MORB compositions, which was formerly interpreted to indicate that a depleted MORB component is not present in the mantle source of the old Emperor Seamounts (Frey et al., 2005; Huang et al., 2005a).

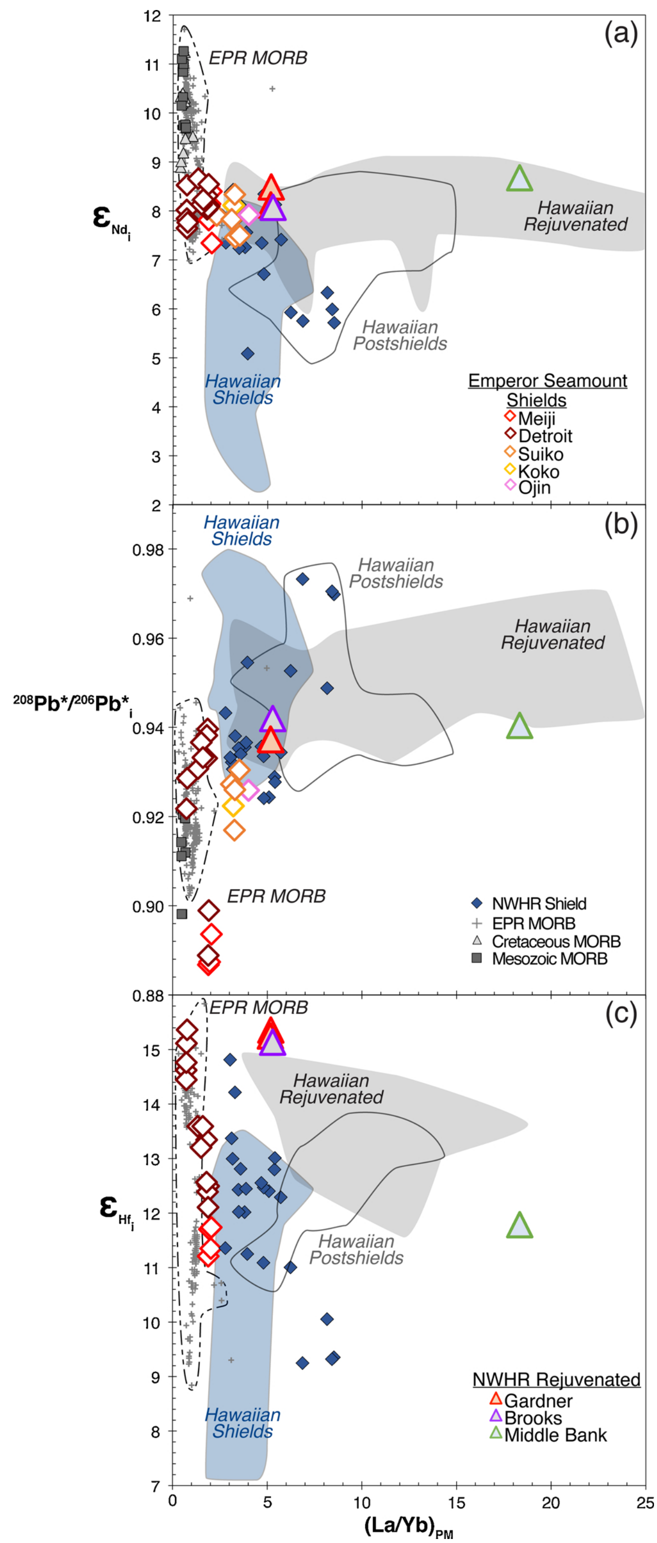

(caption on next page)

Fig. 10. Isotopic ratios versus primitive mantle-normalized La/Yb for the Hawaiian-Emperor chain.
(a) epsilon Nd (b) $^{208}Pb^{*}/^{206}Pb^{*}$ (c) epsilon Hf versus primitive mantle-normalized La/Yb (normalizing values from McDonough and Sun, 1995; refer to Fig. 5d for $^{87}Sr/^{86}Sr$ versus La/Yb). Two SE error bars on new NWHR analyses are smaller than data points. Aside from enriched Loa Hawaiian shield basalts (e.g., West Kaʻena, Koʻolau, Lānaʻi, Kahoʻolawe), all Hawaiian Island and NWHR basalts (e.g., preshield, shield, postshield, rejuvenated) plot within a limited isotopic range. This is regardless of variations in the degree of melting (approximated by the La/Yb ratio; a higher La/Yb indicates lower degrees of partial melting; Hofmann and Farnetani, 2013). EPR MORB plots outside of the Hawaiian plume-derived isotopic range because it has a different mantle source that does not participate in Hawaiian volcanism (Schilling et al., 1983; Schilling, 1991; Hofmann, 2014). Also outside of the Hawaiian plume range are the oldest Emperor Seamounts, a result of differences in source of Emperor Seamount basalts (e.g., interaction with a mid-ocean ridge) from purely plume-derived basalts. The fields and data sources for the Hawaiian Islands are the same as in Fig. 1 and EPR MORB and Emperor Seamount data is the same as in Fig. 2. References for Hawaiian Island postshield data are from Feigenson et al., 1983; Chen et al., 1990, 1991; Frey et al., 1990; Blichert-Toft et al., 1999; Stracke et al., 1999; Cousens et al., 2003; Xu et al., 2005, 2007; Garcia et al., 2010; Greene et al., 2010; Hanano et al., 2010; and Cousens and Clague, 2015. All isotopic data is normalized to the same standard values.

However, recent studies of the geochemical composition of a greater spatial coverage of the East Pacific Rise shows considerably more heterogeneity than was previously known (e.g., Mallick et al., 2019). In addition to the unradiogenic Pb observed at the Garrett Transform Fault of the EPR ($^{206}Pb/^{204}Pb < 17.462$), low $^{206}Pb/^{204}Pb$ was noted between 15°37′N and 15°47′N where the Mathematician Seamounts cross the EPR, and in isolated samples scattered along the entire strike of the EPR (Wendt et al., 1999; Mougel et al., 2014, 2015; Mallick et al., 2019). Furthermore, Mesozoic MORB is a more plausible end-member for Emperor Seamount basalts than EPR MORB because the Hawaiian mantle plume may have been interacting with the Kula-Pacific-Izanagi spreading ridge system at around 70 Ma (Fig. 11; Mammerickx and Sharman, 1988; Caplan-Auerbach et al., 2000; Cottrell and Tarduno, 2003; Norton, 2007; Miyazaki et al., 2015). Mesozoic MORB is more depleted than modern Pacific MORB in isotopic and trace element composition because it represents the Pacific upper mantle before the mid-Cretaceous magmatic event injected heterogeneous, plume-derived material into the Pacific upper mantle (Janney and Castillo, 1997; Miyazaki et al., 2015).

The oldest Emperor Seamounts were erupted near the Kula-Pacific and Pacific-Izanagi mid-ocean ridges, fast spreading ridges (estimated at 18 cm/year for the Kula-Pacific; Sleep, 2007) active between ~75-81 million years (Fig. 11; Lonsdale et al., 1993; Norton, 2007; Wright et al., 2016). Recent plate reconstructions place the Hawaiian mantle plume near the active Kula—Pacific mid-ocean ridge during emplacement of Meiji, which is best estimated as older than Detroit Seamount (> 81 Ma; Keller et al., 1995; Müller et al., 2016; Wright et al., 2016). The location of Kula—Pacific spreading is contentious; it likely started in the west-east direction at the Chinook Trough and was most active at ~80 Ma (Fig. 11; Woods and Davies, 1982; Lonsdale, 1988; Mammerickx and Sharman, 1988; Atwater et al., 1993; Wright et al., 2016; MacLeod et al., 2017). The Emperor Trough has also been identified as a potential failed rift that would have been active at this time (Woods and Davies, 1982; MacLeod et al., 2017). Chinook Trough spreading (i.e., the east-west oriented Kula—Pacific mid-ocean ridge at the southern edge of the Kula Plate) had ceased by ~79 Ma, after the emplacement of Detroit (Mammerickx and Sharman, 1988). Active north-south oriented Kula-Pacific mid-ocean ridge spreading moves farther from the Hawaiian plume as the section from Jimmu to Suiko is erupted, resulting in the more plume-like geochemical signature of Emperor Seamount basalts with time until spreading at the Kula—Pacific ridge ceased by ~41 Ma (Fig. 11; Lonsdale, 1988).

Initiation of plumes and mid-ocean ridges may be associated in time and space, which has been used to suggest that mid-ocean ridges tend to "jump" towards plumes and that plumes tend to "flow" towards ridges, even against the direction of plate motion (Ito et al., 2003; Mittelstaedt and Ito, 2005; Taylor, 2006; Verzhbitskii et al., 2006; Janney and Castillo, 1997; Kingsley et al., 2007; Konter and Jackson, 2012; Geldmacher et al., 2013; Heydolph et al., 2014; Le Saout et al., 2014; Whittaker et al., 2015). Globally, there is evidence that hot material flows between ridges and plumes (Schilling, 1991; Dalton et al., 2014; Whittaker et al., 2015), evidenced by the volcanic lineaments that connect mid-ocean ridges and plumes (Small, 1995; Dyment, 1998; Weis and Frey, 2002; Kopp et al., 2003; Mittelstaedt and Ito, 2005; Vlastélic and Dosso, 2005; Kingsley et al., 2007; Harpp et al., 2014). In addition, MORB erupted near the estimated prior locations of plumes are geochemically more enriched than N-MORB (hence E-MORB; Schilling et al., 1983; Hofmann, 2014) and the associated plume seamounts are more depleted, reflecting mutual interaction (Wendt et al., 1999; Mittelstaedt and Ito, 2005; Janney and Castillo, 1997; Kingsley et al., 2007; Konter and Jackson, 2012; Geldmacher et al., 2013; Le Saout et al., 2014; Mougel et al., 2014, 2015). The isotopic and trace element systematics of the Cretaceous Emperor Seamounts record signatures of interaction with a mid-ocean ridge, and are very plausibly a result of plume-ridge interaction of the Hawaiian plume with the Kula-Pacific-Izanagi spreading ridge system (Keller et al., 2000).

6.4. The depleted mantle component in Hawaiian rejuvenated magmatism

The unique composition of Hawaiian rejuvenated basalts is attributed to the presence of distinctive compositional components in the mantle source along with dynamic mechanisms that are specific to the rejuvenated volcanic stage. Proposed explanations for the genesis of Hawaiian rejuvenated basalts include melting the lithosphere currently underneath Hawaiian volcanoes (Chen and Frey, 1983; Chen et al., 1990, 1991), a depleted MORB source recently metasomatized by Hawaiian plume melts (Chen and Frey, 1983, 1985; Feigenson, 1984; Clague and Dalrymple, 1987; Yang et al., 2003), mixing between low degree melts from the plume and a MORB source (Roden et al., 1984; Reiners and Nelson, 1998; Dixon et al., 2008; Béguelin et al., 2019), secondary melting of plume stem material as the result of secondary uplift of asthenosphere from flexure of the lithosphere under the weight of the currently building shield (Ribe and Christensen, 1999; Bianco et al., 2005), an entrained upper (Lassiter et al., 2000; Fekiacova et al., 2007) or lower (Hofmann and Farnetani, 2013) mantle sheath on the exterior of the Hawaiian mantle plume; melting of pyroxenite on the edges of the plume (Ballmer et al., 2011; Garcia et al., 2016); or a depleted plume matrix that does not contribute appreciably, or is overwhelmed by, the isotopic and trace element characteristics of the more enriched components (Frey et al., 2005).

There are several lines of evidence that suggest that the depleted component in rejuvenated basalts does not originate from melting of previously melted Hawaiian plume components that have not been metasomatized subsequent to shield and postshield melting and prior to rejuvenated melting. First, the highly incompatible trace element concentrations of rejuvenated basalts coupled with their depleted isotopic signature (e.g., high Hf and Nd isotope ratios coupled with low Sr isotope ratios) cannot be reconciled by re-melting of the shield-stage source (Clague and Frey, 1982; Feigenson, 1984; Yang et al., 2003; Fekiacova et al., 2007; Garcia et al., 2010). Second, postshield basalts are thought to represent the continued melting of the Hawaiian plume shield-stage source (Hanano et al., 2010; Béguelin et al., 2019). The limited range of isotopic composition in rejuvenated basalts compared to postshield basalts suggests that rejuvenated basalts are not formed by re-melting of the same mantle source. Third, rejuvenated basalts exhibit high volatile concentrations, strong evidence that their source has not been depleted by previous melting during the shield and postshield volcanic stages (Frey et al., 2000; Dixon et al., 2008; Hofmann and Farnetani, 2013). Finally, the highly alkalic composition of rejuvenated

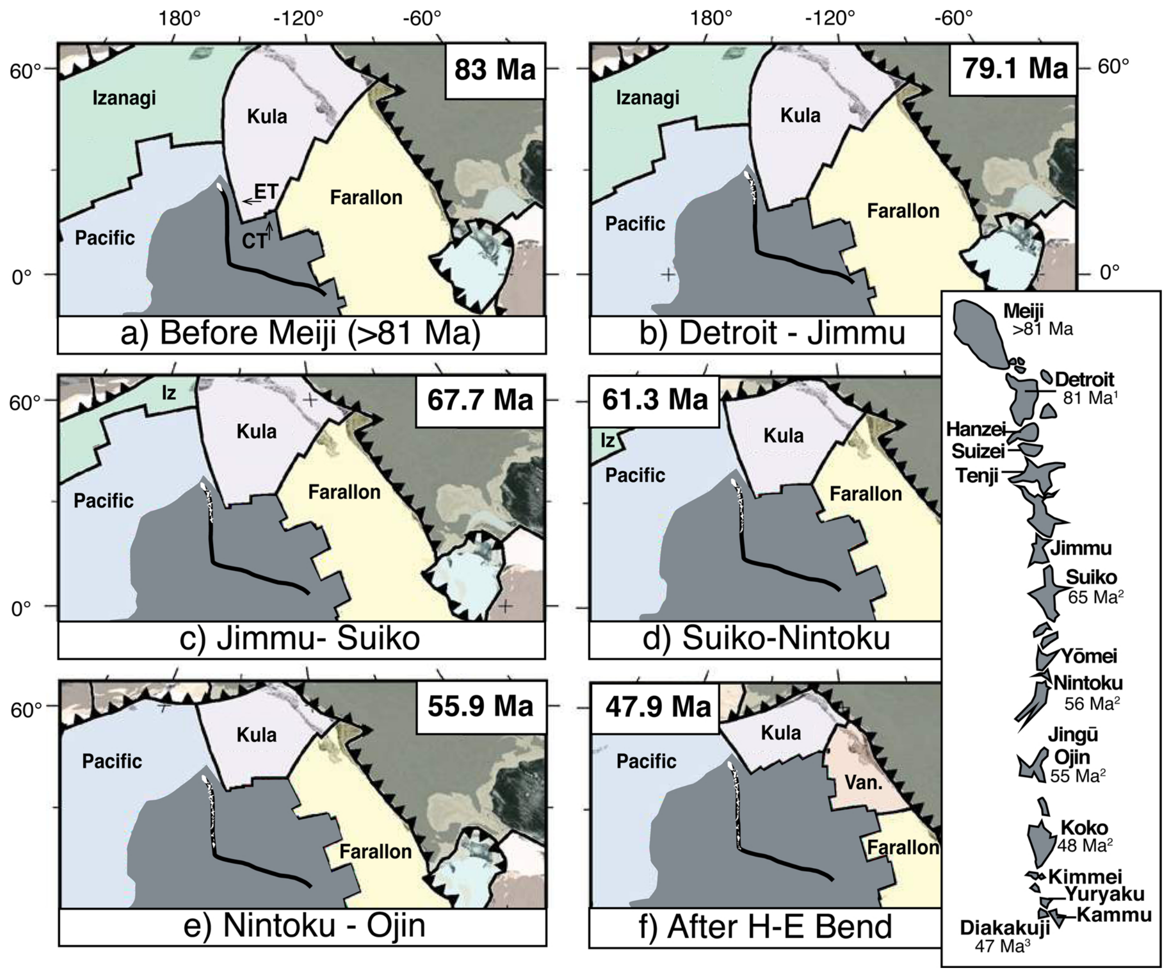

Fig. 11. Plate Organization During Emperor Seamount Emplacement.
This figure is modified from Wright et al., 2016 and presents their plate reconstruction of the circum-Pacific region during Late Cretaceous and Early Cenozoic based upon recent, better resolution fracture zone traces, magnetic lineations, and new satellite bathymetry. The grey "plate" in the center of the diagrams represents presently preserved oceanic crust and is a part of the Pacific Plate. The black line represents the current location of the Hawaiian-Emperor chain, and the white dots that appear on this line represent the extent of Emperor Seamounts that existed at the time period in each panel. The inset figure is a generalized map of the Emperor Seamounts traced from the 2-minute Gridded Global Relief Data ETOPO2v2 satellite altimetry dataset (U.S. Department of Commerce, National Oceanic and Atmospheric Administration, National Geophysical Data Center, 2006; downloaded March 2014). Ages for the Emperor Seamounts are as follows: 1 – Keller et al., 1995; 2 – Clague and Dalrymple, 1987; 3 – O'Connor et al., 2013. (a) Chron 34, or ~83 Ma. According to this reconstruction, Meiji was erupted near the active Kula—Pacific mid-ocean ridge. Meiji has never been accurately dated and is best estimated as older than Detroit Seamount (> 81 Ma; Keller et al., 1995). It is possible that there were older Hawaiian volcanoes than Meiji that have since been either accreted to Kamchatka or subducted in the Kamchatka trench (Portnyagin et al., 2008). The location of Kula—Pacific spreading is contentious; it likely started in the west-east direction at the Chinook Trough (abbreviated at CT; Lonsdale, 1988; Mammerickx and Sharman, 1988; Atwater et al., 1993; Wright et al., 2016; MacLeod et al., 2017). The Emperor Trough (abbreviated as ET) is either a proposed failed rift or a transform fault (i.e., not identified as a full-fledged spreading ridge in the extinct-ridge analysis by MacLeod et al., 2017). Potential rifting was most active during initiation of the Kula—Pacific spreading ridge at ~80 Ma (Woods and Davies, 1982). (b) Chron 33old or 79.1 Ma; the emplacement of the Cretaceous Emperor Seamounts (i.e., Detroit, Hanzi, Suizei, Tenji) were also erupted near the Kula—Pacific mid-ocean ridge; it has been proposed that Chinook Trough spreading (i.e., the east-west oriented Kula—Pacific mid-ocean ridge at the southern edge of the Kula Plate) had ceased by ~79 Ma, after the emplacement of Detroit (Mammerickx and Sharman, 1988). (c) Chron 31young or 67.7 Ma; active mid-ocean ridge spreading is farther from the Hawaiian plume as the section from Jimmu to Suiko is erupted, resulting in more plume-like geochemical signature of Suiko basalts. (d) Chron 27old or 61.3 Ma; the active Hawaiian mantle plume is located still farther from spreading centers. (e) Chron25young or 55.9 Ma; the Izanagi—Pacific mid-ocean ridge subducted; the Hawaiian plume formed Nintoku to Ojin Seamounts far from active spreading centers. (f) Chron 21old or 47.9Ma; Although it is debated, this is roughly synchronous or directly after the bend in the Hawaiian-Emperor chain (Dalrymple and Clague, 1976; O'Connor et al., 2013; Sharp and Clague, 2006a, 2006b). All of the Emperor Seamounts are now formed, and the active plume is located far from active mid-ocean ridge spreading (the Kula—Pacific spreading ridge ceased by ~41 Ma; Lonsdale, 1988).

basalts and mostly MgO rich (> 10 wt% MgO) cannot be produced by fractionation of shield or postshield composition magmas, and instead requires a different source (Feigenson, 1984; Clague and Frey, 1982). The mantle plume edges represent the best candidates for a pure rejuvenated source because: 1) rejuvenated basalts are typically produced after the volcano has moved hundreds of kilometers away from the active plume stem (Duncan et al., 1994; White and Duncan, 1996; Sherrod et al., 2007); 2) the lower temperatures of the plume edge allow the low degrees of melting required by forward modeling of rejuvenated basalt trace and major element concentrations (Garcia et al., 2010); and 3) dynamic models have shown that margins of the plume are likely the main region of rejuvenated-stage melting (Hofmann and Farnetani, 2013). Thus, it is plausible that rejuvenated basalts originate from the edge of the Hawaiian mantle plume by melting mantle material that did not participate in either shield or postshield volcanism. Mantle material that meets the above requirements is entrained material from either the lower or upper mantle (Farnetani and Richards, 1995). If the source of rejuvenated basalts is entrained mantle, can geochemistry distinguish a depleted upper mantle source from a depleted lower mantle source?

Previous investigation of rejuvenated basalts from Kaua‘i and O‘ahu eliminated MORB-related lithosphere as a possible source component in rejuvenated basalts based on Pb isotope systematics of the Kōloa and Honolulu Volcanics that did not define mixing lines with ODP Site 843 or EPR MORB fields (Fekiacova et al., 2007; Garcia et al., 2010; Hanano et al., 2010). Data on abyssal peridotites and global MORB samples however, suggests that the composition of the upper mantle may be more heterogeneous than previously thought (Warren et al., 2009; Salters et al., 2011; Stracke et al., 2011; Parai et al., 2012; Sanfilippo et al., 2019). The upper mantle may store ultra-depleted reservoirs that are effectively invisible under normal melting conditions and may change with time and influx of deep plume material, such as with the progressive enrichment of the Pacific upper mantle during the mid-Cenozoic magmatic event (Larson, 1991; Janney and Castillo, 1997; Ito and Clift, 1998; Salters et al., 2011; Byerly and Lassiter, 2014). This ultra-depleted upper mantle component is characterized by very unradiogenic Pb isotope ratios (down to $^{206}Pb/^{204}Pb$ ~16.5) and extremely high Hf (epsilon Hf of 20–40) and Nd (epsilon Nd of 10–20) isotopic compositions (Malaviarachchi et al., 2008; Salters et al., 2011). These isotopic compositions are rare because of their extremely refractory nature; these rocks have already been melted at least once, which fractionated the Lu-Hf from the Sm-Nd isotopic systems as Lu is retained in mantle garnet while Sm enters the melt (Salters et al., 2011). Over time, these processes result in oceanic lithosphere with highly radiogenic Hf isotopic compositions coupled with Nd isotopic compositions similar to the range observed in MORB. The highly radiogenic Hf isotope reservoirs are not related to oceanic lithosphere that melted to create the current Pacific oceanic crust (which has a maximum age ~200 Ma), as this lithosphere is not old enough to develop the appropriately radiogenic Hf isotopic compositions (the half-life of ^{176}Lu to radiogenically decay into ^{176}Hf is roughly 36 Ga; Luo and Kong, 2006). The high Hf isotopic compositions observed in Hawaiian xenoliths from Ka‘ula and O‘ahu (Bizimis et al., 2005, 2007, 2013) and high Hf isotope ratios in NWHR rejuvenated magmatism (Fig. 9), suggest either that old recycled oceanic lithosphere is present in the Hawaiian source or that residual, ancient, highly depleted mantle resides in the Pacific upper mantle. Dynamic modeling of the Hawaiian and Mauritius plume systems has shown that upper mantle entrained materials cannot reach temperatures high enough to partially melt (Ribe and Christensen, 1999; Paul et al., 2005). Therefore, depleted material with high Hf isotope ratios from recycled oceanic lithosphere is probably sampled from the lower mantle (Paul et al., 2005; Hofmann and Farnetani, 2013). The presence of ancient recycled lithosphere in the Hawaiian plume is supported by Re-depletion ages of two billion years in O‘ahu peridotite xenoliths (Bizimis et al., 2007), and the low Os isotope ratios of some Hawaiian basalts (Lassiter and Hauri, 1998). However, although it is more likely such an old depleted source would be intrinsic to the plume because it must be centrally located to be heated enough for melt production, it is possible that this component is ubiquitous in the mantle and mostly undetected because it infrequently melts without becoming diluted by more fertile compositions. The presence of depleted components in the upper mantle are supported by the extremely depleted major element and $^{143}Nd/^{144}Nd$ isotope ratios of abyssal peridotites (Warren et al., 2009; Warren, 2016), high Hf isotope ratios in some MORB (Liu et al., 2008; Salters et al., 2011), and melting models that show such depleted components in the upper mantle can contribute to MORB (Byerly and Lassiter, 2014). However, linking mantle components to a reservoir in either the upper or lower mantle is complicated by the inherent uncertainties associated with estimating the composition of the lower mantle, which has never been directly sampled.

Evidence for the existence of different depleted sources for Hawaiian rejuvenated lavas and Cretaceous Emperor Seamount lavas have been presented above. However, it is important to point out that these two different sources are likely themselves a result of mixing between the Hawaiian mantle plume and the upper mantle MORB source for the Emperor Seamounts, and are potentially a mix of several mantle lithologies associated with the Hawaiian plume for the rejuvenated stage. Researchers have suggested that the Hawaiian rejuvenated component itself is a result of mixing between different sources, varying degrees of metasomatism from a variety of sources, or extremely small degrees of melting from a depleted source (Chen and Frey, 1983, 1985; Feigenson, 1984; Roden et al., 1984; Clague and Dalrymple, 1987; Reiners and Nelson, 1998; Yang et al., 2003; Dixon et al., 2008; Béguelin et al., 2019).

Furthermore, the above discussion assumes that the source of Hawaiian rejuvenated lavas is represented by a mantle component that is typified by the trace element and isotopic characteristics of erupted rejuvenated lavas. However, the mechanism of forming rejuvenated lavas may be complicated by metasomatism, melt-rock mixing, or melt-melt mixing, which may result in refertilization of a previously melted mantle source with the high incompatible trace element and high volatile concentrations observed in rejuvenated lavas (Chen and Frey, 1983, 1985; Feigenson, 1984; Roden et al., 1984; Clague and Dalrymple, 1987; Reiners and Nelson, 1998; Yang et al., 2003; Dixon et al., 2008; Béguelin et al., 2019). These models could also explain the unique characteristics of Hawaiian rejuvenated volcanism, although metasomatism is a highly heterogeneous process that would likely not produce such homogenous isotopic compositions for ~12.5 Ma as observed in both NWHR and Hawaiian rejuvenated lavas. Recent observations of oceanic island melt inclusions with highly depleted Sr and Nd isotope ratios suggest depleted components are frequently overlooked because of dilution by even tiny amounts of enriched melts (Rudge et al., 2013; Genske et al., 2019; Neave et al., 2019; Stracke et al., 2019). This implies that the presence of depleted mantle components may be shielded from observation in most mantle-derived melts and suggests that the consistent, depleted isotopic composition of Hawaiian rejuvenated basalts are even more remarkable, especially considering metasomatic fluids or melts derived from the Hawaiian plume will carry more enriched isotopic signatures. The debate on the origin of the depleted component typical of Hawaiian rejuvenated lavas is still, therefore, unsettled and we suggest the analysis of Sr and Nd isotopes in melt inclusions of Hawaiian rejuvenated basalts may have the potential to shed more understanding into the partial melting, melt mixing, and crystal differentiation processes that create the enigmatic rejuvenated compositions.

6.5. Hawaiian rejuvenated volcanism compared to other oceanic islands

To generate rejuvenated magmas with depleted isotopic compositions and enriched incompatible trace elements, excess heat must be retained in areas of the mantle away from the active plume stem and/or decompression melting initiated downstream of the active plume stem (Clague and Dalrymple, 1987; Sleep, 1990; Sherrod et al., 2007; Clague and Sherrod, 2014). The Hawaiian swell may be isostatically uplifted by the Hawaiian mantle plume itself, causing thermal rejuvenation of the lower ~50 km of the lithosphere downstream of the active plume (Li et al., 2004), and chemical buoyancy due to underplating (Leahy et al., 2010; Sleep, 1990; Wessel, 2016). This uplift, coupled with the weight of the shield volcano building downstream, may provide the necessary critical conditions to produce rejuvenated volcanism as observed along the NWHR and Hawaiian Islands. Furthermore, both mantle potential temperature and magmatic flux have generally increased along the NWHR starting at about Midway (Van Ark and Lin, 2004; Vidal and Bonneville, 2004; Tree, 2016; Wessel, 2016). Higher magmatic flux and higher mantle potential temperature will both increase the amount of heat supplied to the base of the lithosphere and the mass and volume of Hawaiian volcanoes. Presumably, greater volumes of rejuvenated magmatism would be generated under these conditions, suggesting there may be a relationship between the increase in the Hawaiian mantle plume flux along the NWHR and the volume of rejuvenated basalts produced. For example, the Northern Hawaiian Islands, where magmatic flux increases exponentially (Van Ark and Lin, 2004; Vidal and Bonneville, 2004; Wessel, 2016), experienced rejuvenated volcanism in an unprecedented volume (Holcomb and Robinson, 2004; Sherrod et al., 2007; Cousens and Clague, 2015). It is also possible that Hawaiian rejuvenated volcanism is only produced on mature lithosphere with sub-lithospheric small-scale convection that develops in oceanic crust ≥70 Ma (Doin and Fleitout, 1996; Sleep, 2011 and references therein). Small-scale convection is a process proposed to be the major mechanism limiting the thickness of ocean crust, and does so by upwelling mantle eroding the base of the lithosphere. This potential erosional topography on the base of the lithosphere may create zones of greater mantle upwelling and decompression melting away from the active Hawaiian plume that is not entirely predictable, a similarity with the occurrences of Hawaiian rejuvenated volcanism (Fig. 1; Ballmer et al., 2011).

The conditions described above are different between Hawai'i and other oceanic islands, where rejuvenated volcanism, if present, may be caused by a variety of mechanisms and is potentially more difficult to distinguish from the shield stage because the majority of the lavas erupted at other OIB locations, regardless of volcanic stage, are alkalic in composition and may have complex volcanic histories with both longer durations of volcanism than is typical at a Hawaiian volcano (typically ~1 million years for the shield stage) and episodes of post-shield and rejuvenated volcanism of varying composition and duration (Garcia et al., 2015; Rodriguez-Gonzalez et al., 2018; Haase et al., 2019). Rejuvenated volcanic rocks have been observed in Samoa, Society, the Marquesas, the Canary Islands, and Mauritius (see Fig. 12 and references in the supplementary information for compiled data). The evolution from shield to postshield to rejuvenated volcanism on the Marquesas is marked by an evolution from low to high Sr and Pb isotope compositions, opposite to what is observed in Hawai'i. This transition is attributed to greater melt interaction between the weak Marquesas' plume and the lithosphere (Woodhead, 1992). The Islands of Samoa erupted rejuvenated basalts that are enriched in trace elements with depleted lithospheric isotopic compositions. This geochemical signature was explained by a tectonic, subduction-aided flexural bending and melting of the lithosphere beneath the island, also very different from Hawai'i (Fig. 12; Hawkins and Natland, 1975; Natland, 1980; Hauri and Hart, 1993; Workman et al., 2004; Konter and Jackson, 2012; Jackson et al., 2014; Reinhard et al., 2019). The Canaries have a significantly longer duration of postshield and rejuvenated volcanism than Hawai'i because of the slow moving African plate (< 2 cm/year), compared to the fast moving Pacific plate (9–10 cm/year; Paris et al., 2005). Although the Canary Islands are underlain by a mantle plume that has been seismically imaged to at least mid-mantle depths, the five million years of post-erosional volcanism on Gran Canaria, producing significantly evolved lava compositions including phonolites and ignimbrites, are very dissimilar to Hawaiian style rejuvenated volcanism (Wolff and Palacz, 1989; Cousens et al., 1990, 1993; Hoernle and Schminke, 1993; Johansen et al., 2005; Montelli et al., 2006). Rejuvenated volcanism on the Society Islands is remarkably similar to Hawai'i with more depleted isotope compositions than previous volcanic phases and major and trace element compositions that cannot result from remelting of the same mantle source as earlier volcanics (Cheng et al., 1993). Society rejuvenated volcanism is proposed to originate from an entrained lower mantle sheath because of the trace element concentrations that are enriched relative to the depleted mantle, but the small number of analyses of rejuvenated lavas preclude an in depth analysis (Cheng et al., 1993; White and Duncan, 1996; Hildenbrand et al., 2004). On Mauritius, the presence of rejuvenated basalts is proposed to reflect secondary uplift, a process similar to the dynamic flexure model proposed for Hawai'i (Ribe and Christensen, 1999; Bianco et al., 2005; Paul et al., 2005; Moore et al., 2011). Also similar to Hawai'i, dynamic models of Mauritius do not support entrainment of upper mantle as the source of rejuvenated basalts because entrained mantle is not heated sufficiently to melt and would require unrealistic decompression of the mantle (corresponding to ~15 km of uplift; Paul et al., 2005).

Rejuvenated compositions have limited isotopic ranges relative to the larger range of variations observed in shield stage basalts, aside from the Canary Islands, suggesting that although the mechanisms of generating rejuvenated volcanism are hypothesized to be different among OIBs, the compositions of the depleted components tend to be less heterogeneous than those present during the shield stage (Fig. 12). This observation in not new, as enriched components present in OIB have typically been invoked to explain the different "flavors" of OIBs (i.e., HIMU, EM I, EM II) and most global OIBs present variations in geochemistry that coalesces at a common mantle component (i.e., the focal zone, FOZO, or prevalent mantle, PREMA; Zindler and Hart, 1986; Hanan and Graham, 1996; Stracke, 2012; Stracke et al., 2005). It is important to note, however, that the rejuvenated lavas erupted at different oceanic islands do not erupt depleted components of the same composition, suggesting either that depleted components in the mantle vary in either composition and time-integrated history (as enriched components do), or that a global depleted composition is consistently overprinted by the enriched components associated with each mantle plume.

The rejuvenated lavas erupted at Hawai'i, Samoa, and the Canary Islands present compositions farthest from PREMA, whereas Marquesas, Society, and Mauritius cluster around this common mantle composition (Fig. 12). If the Canary Islands are excluded from the comparison because the duration and evolved composition indicate a more complicated mechanism for the formation of rejuvenated lavas at this oceanic island, it is interesting to point out that Hawai'i and Samoa are both sourced by mantle plumes with unique geophysical and geochemical characteristics. For example, the maximum primitive He isotope anomalies associated with Hawai'i ($^3He/^4He$ = 35.3 R_A) and Samoa ($^3He/^4He$ = 33.8 R_A) are higher than Society ($^3He/^4He$ = 17.0 R_A), Marquesas ($^3He/^4He$ = 14.4 R_A), the Canary Islands ($^3He/^4He$ = 9.7 R_A), and Réunion (used as a proxy for Mauritius, $^3He/^4He$ = 13.6 R_A; Jackson et al., 2017 and references therein), suggesting a deeper origin for Hawai'i and Samoa relative to Society, Marquesas, Canary, and Mauritius Islands. The relative strength of the mantle plumes generating these OIBs are also quite different, with the magnitude of plume buoyancy flux of Hawai'i and Samoa being much higher than Society, Marquesas, Canary, and Mauritius, and the size of the seismic velocity anomaly at depth beneath the surface expression of the plume is greater underneath Hawai'i and Samoa than the other four plumes (Jackson et al., 2017). Further modeling is beyond the scope of this review, but it is interesting to hypothesize that the strength of the plume supplying an oceanic island may affect the amount of entrained depleted compositions of different time-integrated histories and also hotter, stronger plumes may supply the excess heat necessary to melt more refractory depleted compositions, controlling the chemistry of rejuvenated lavas.

The Hawaiian mantle plume has the highest magmatic flux and has one of the highest mantle potential temperatures of any oceanic islands worldwide (Van Ark and Lin, 2004; Vidal and Bonneville, 2004; Putirka, 2005; Wessel, 2016). It is also one of the only oceanic islands to erupt mainly tholeiitic rather than alkalic basalt compositions (Sleep, 1990; Courtillot et al., 2003; Chauvel et al., 2012; Haase et al., 2019). The location of Hawai'i far from any active tectonic setting eliminates other (i.e., non-plume related) tectonic mechanisms to account for the formation of rejuvenated basalts. Instead, the high temperature and magmatic flux of Hawaiian plume may result in the mantle melting more readily under Hawai'i than at other oceanic islands, where a more fusible plume component is necessary to produce rejuvenated volcanism (e.g., the Marquesas; Woodhead, 1992). Although the volume and distribution of rejuvenated-stage basalts along the NWHR and

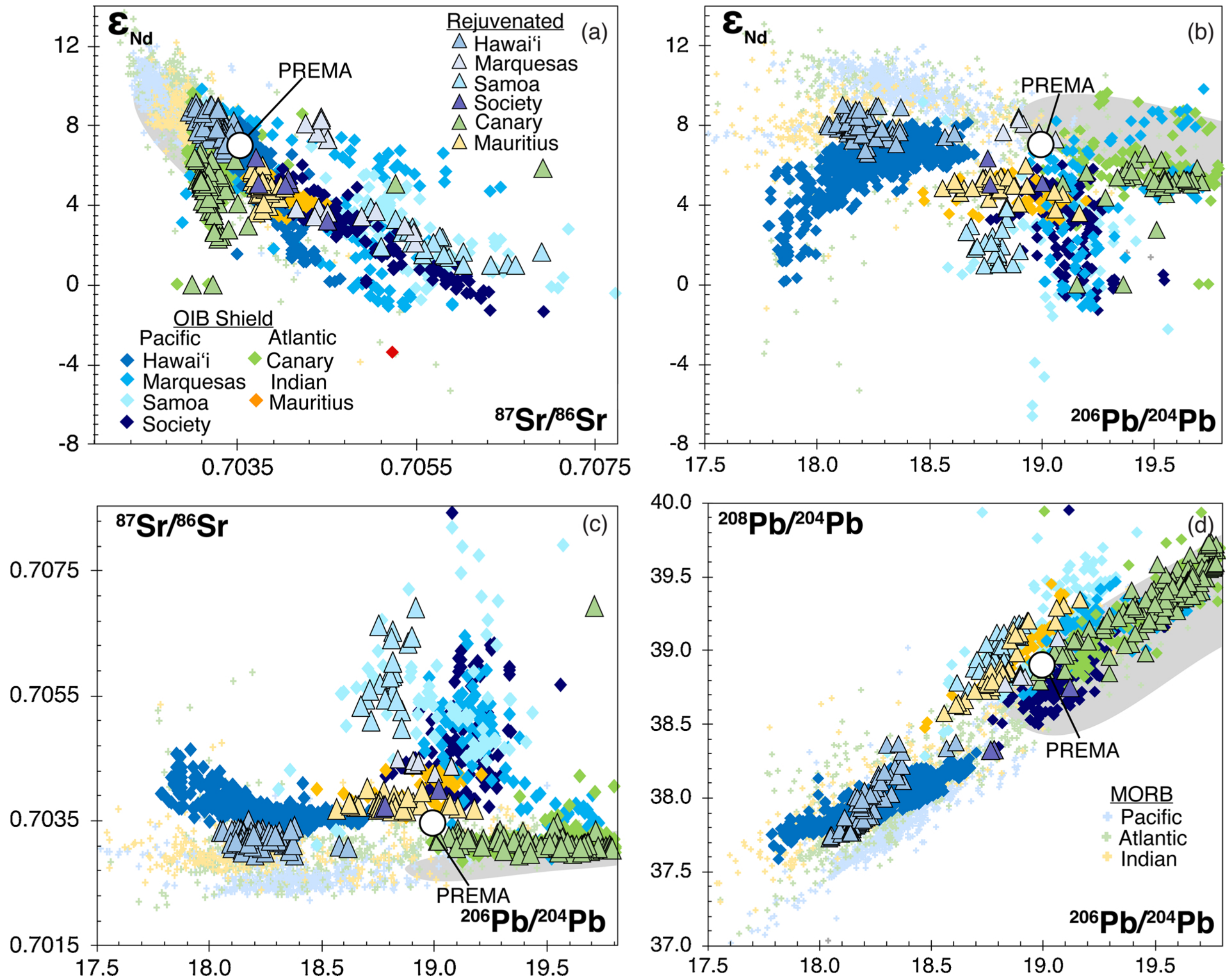

Fig. 12. Isotopic Variation of Global Oceanic Island Rejuvenated Basalts.
(a) epsilon Nd versus $^{87}Sr/^{86}Sr$ (b) epsilon Nd versus $^{206}Pb/^{204}Pb$ (c) $^{87}Sr/^{86}Sr$ versus $^{206}Pb/^{204}Pb$ (d) $^{208}Pb/^{204}Pb$ versus $^{206}Pb/^{204}Pb$ of global oceanic islands with a documented rejuvenated volcanic stage. The fields and data sources for the Hawaiian Islands are the same as in Fig. 1 and EPR MORB and Emperor Seamount data sources are the same as in Fig. 2. The sources of global OIB shield stage and rejuvenated lavas are listed in the supplementary information and all isotopic data is renormalized to the same standard values. The white circle indicates the location of PREMA (Pb isotope composition is form Hanan and Graham, 1996 and the Nd and Sr isotope compositions are from Zindler and Hart, 1986). The shaded grey field indicates the PREMA field of Stracke, 2012.

Emperor Seamounts is still largely unconstrained (see section 2 above), we hypothesize that the increased strength of the Hawaiian plume starting at ~30 Ma is responsible for greater volumes of rejuvenated volcanism along the younger end of the Hawaiian-Emperor chain observed by the current sampling resolution. The volume of rejuvenated volcanism on the NWHR may be quantified in the future by high-resolution sidescan-sonar imagery similar to studies of the seafloor around the Hawaiian Islands (Holcomb and Robinson, 2004; Garcia et al., 2008). Additional sampling and geochronology of NWHR and Emperor Seamounts will also further constrain the spatial frequency of Hawaiian rejuvenated volcanism and may help refine the possible connection between plume flux and rejuvenated volcanism.

7. Conclusion

This study investigated the geochemistry of rejuvenated-stage volcanism sampled along the NWHR and compared the geochemical signatures of the depleted components present in Hawaiian basalts along the entire Hawaiian-Emperor chain. NWHR rejuvenated basalts are virtually indistinguishable in trace element and isotopic composition from Hawaiian Island rejuvenated basalts, an observation that extends the homogeneity and the existence of the rejuvenated component up to ~12.5 Ma. This homogeneous rejuvenated component is different from the depleted component observed in the oldest Emperor Seamounts in both trace element systematics and isotopic compositions. The oldest Emperor Seamount basalts document the geochemically depleted imprint of a plume-ridge interaction (e.g., low $^{87}Sr/^{86}Sr$ and $^{208}Pb^{*}/^{206}Pb^{*}$ with high $^{176}Hf/^{177}Hf$), while the source of rejuvenated basalts along the NWHR is likely entrained lower mantle located on the edge of the Hawaiian mantle plume. The radiogenic Hf isotope compositions of NWHR and Hawaiian rejuvenated basalts suggest that the depleted component may contain ancient recycled oceanic lithosphere. Increasing the sampling resolution of rejuvenated basalts from the NWHR will further constrain their mechanism of formation and contribute to determining the geochemical origins of this enigmatic volcanic stage. Here we present a simple interpretation of geochemical data within the context of geodynamic and geophysical studies to propose a hypothesis about the presence and source of two different Hawaiian depleted components. We emphasize that this does not preclude other more complicated models of how Hawaiian rejuvenated volcanism is formed and that there will be much greater value in future studies if they bridge the gaps between geochemistry, geophysics, and geodynamics.

Acknowledgements

Our thanks go to Kathy Gordon, Vivian Lai, Bruno Kieffer, and Liyan Xing for assistance analyzing Pb-Hf-Nd-Sr isotopes and trace element compositions. We are grateful to D. Clague and J. Tree for some of the samples used in this study and thank Dennis Geist for major and trace element data for the rejuvenated sample from Middle Bank. Discussions with Nicole Williamson, Catherine Armstrong, Diane Hanano, and James Scoates contributed greatly to the manuscript, as did constructive reviews from William White, Michael Bizimis, Marcel Regelous, Shichun Huang, and three anonymous reviewers. We would also like to thank Catherine Chauvel for discussions related to this work and for careful editorship. This work was supported through NSF grants EAR-1219955 and OCE-1834758 to M. O. Garcia, NSERC Discovery Grant to D. Weis, and a University of British Columbia Four Year Fellowship to L. Harrison. This work was performed under the auspices of the U.S. Department of Energy by Lawrence Livermore National Laboratory under Contract DE-AC52-07NA27344. LLNL-JRNL-770460.

Appendix A. Supplementary data

Supplementary data associated with this article can be found, in the online version, at http://dx.doi.org/10.1016/j.chemgeo.2019.119324.

References

Abouchami, W., Hofmann, A.W., Galer, S.J.G., Frey, F.A., Eisele, J., Feigenson, M., 2005. Lead isotopes reveal bilateral asymmetry and vertical continuity in the Hawaiian mantle plume. Nature 434, 851–856.
Atwater, T., Sclater, J., Sandwell, D., Severinghaus, J., Marlow, M.S., 1993. Fracture zone traces across the North Pacific Cretaceous quiet zone, and their tectonic implications. Mesozoic Pacific: Geol. Tectonics, and Volcan. 137–154.
Ballmer, M.D., Ito, G., van Hunen, J., Tackley, P.J., 2011. Spatio and temporal variability in Hawaiian hotspot volcanism induced by small-scale convection. Nat. Geosci. 4, 457–460.
Basu, A.R., Faggart, B.E.F., 1996. Temporal isotopic variations in the Hawaiian Mantle Plume: The Lanai anomaly, the Moloka'i fracture zone and a seawater-altered lithospheric component in Hawaiian volcanism. In: In: Basu, A., Hart, S. (Eds.), Earth Processes: Reading the Isotopic Code Vol. 95. American Geophysical Union, pp. 149–159 Geophys. Monogr. Ser.
Béguelin, P., Bizimis, M., McIntosh, E.C., Cousens, B., Clague, D.A., 2019. Source vs processes: unraveling the compositional heterogeneity of rejuvenated-type Hawaiian magmas. Earth Planet. Sci. Lett. 514, 119–129.
Bianco, T.A., Ito, G., Becker, J.M., Garcia, M.O., 2005. Secondary Hawaiian volcanism formed by flexural arch decompression. Geochem. Geophys. Geosyst. 6 (8), Q08009.
Bizimis, M., Sen, G., Salters, V.J.M., 2003. Hf-Nd isotope decoupling in the oceanic lithosphere: constraints from spinel peridotites from Oahu, Hawaii. Earth Planet. Sci. Lett. 217, 43–58.
Bizimis, M., Sen, G., Salters, V.J.M., Keshav, S., 2005. Hf-Nd-Sr isotope systematics of garnet pyroxenites from Salt Lake Crater, Oahu, Hawaii: evidence for a depleted component in Hawaiian volcanism. Geochim. Cosmochim. Acta 69 (10), 2629–2646.
Bizimis, M., Griselin, M., Lassiter, J.C., Salters, V.J.M., Sen, G., 2007. Ancient recycled mantle lithosphere in the Hawaiian plume: osmium-hafnium isotopic evidence from peridotite mantle xenoliths. Earth Planet. Sci. Lett. 257, 259–273.
Bizimis, M., Salters, V.J.M., Garcia, M.O., Norman, M.D., 2013. The composition and distribution of the rejuvenated component across the Hawaiian plume: Hf-Nd-Sr-Pb isotope systematics of Kaula lavas and pyroxenite xenoliths. Geochem. Geophys. Geosyst. 14 (10), 4458–4478.
Blichert-Toft, J., Albarède, F., 1997. The Lu-Hf isotope geochemistry of chondrites and the evolution of the mantle-crust system. Earth Planet. Sci. Lett. 148 (1), 243–258.
Blichert-Toft, J., Frey, F.A., Albarède, F., 1999. Hf isotope evidence for pelagic sediments in the source of Hawaiian basalts. Science 285, 879–882.
Bono, R.K., Tarduno, J.A., Bunge, H.-P., 2019. Hotspot motion caused the Hawaiian-Emperor bend and LLSVPs are not fixed. Nat. Comm. 10, 3370.
Boschi, L., Becker, T.W., Steinberger, B., 2007. Mantle plumes: dynamic models and seismic images. Geochem. Geophys. Geosyst. 8, 1–20.
Brandl, P.A., Regelous, M., Beier, C., Haase, K.M., 2013. High mantle temperatures following rifting caused by continental insulation. Nat. Geosci. 6, 391–394.
Broadley, M.W., Sumino, H., Graham, D.W., Burgress, R., Ballentine, C.J., 2018. Recycled components in mantle plumes deduced from variations in halogens (Cl, Br, and I), trace elements, and $^3He/^4He$ along the Hawaiian-Emperor seamount chain. Geochem. Geophys. Geosyst. 20, 1–18.
Byerly, B.L., Lassiter, J.C., 2014. Isotopically ultradepleted domains in the convecting upper mantle: implications for MORB petrogenesis. Geology 42 (3), 203–206.
Caplan-Auerbach, J., Duennebier, F., Ito, G., 2000. Origin of intraplate volcanoes from guyot heights and oceanic paleodepth. J. Geophys. Res. 105 (B2), 2679–2697.
Chauvel, C., Bureau, S., Poggi, C., 2010. Comprehensive chemical and isotopic analyses of basalt and sediment reference materials. Geostand. Geoanalyt. Res. 53 (1), 125–143.
Chauvel, C., Maury, R.C., Blais, S., Lewin, E., Guillou, H., Guille, G., Rossi, P., Gutscher, M.-A., 2012. The size of plume heterogeneities constrained by Marquesas isotopic stripes. Geochem. Geophys. Geosyst. 13 (1), Q07005.
Chen, C.-Y., Frey, F., 1983. Origin of Hawaiian tholeiite and alkalic basalt. Nature 302, 785–789.
Chen, C.-Y., Frey, F., 1985. Trace element and isotopic geochemistry of lavas from Haleakala volcano, East Maui, Hawaii: implications for the origin of Hawaiian basalts. J. Geophys. Res. 90 (B10), 8743–8768.
Chen, C.-Y., Frey, F.A., Garcia, M.O., 1990. Evolution of alkalic lavas at Haleakala Volcano, east Maui, Hawaii. Contrib. Min. Petrol. 105, 197–218.
Chen, C.-Y., Frey, F.A., Garcia, M.O., Dalrymple, G.B., Hart, S.R., 1991. The tholeiite to alkalic basalt transition at Haleakala Volcano, Maui, Hawaii. Contrib. Min. Petrol. 106, 183–200.
Cheng, Q.C., Macdougall, J.D., Lugmair, G.W., 1993. Geochemical studies of Tahiti, Teahitia and Mehetia, Society Island chain. J. Volcano. Geotherm. Res. 55, 155–184.
Clague, D., Dalrymple, B., 1987. The Hawaiian-Emperor Volcanic chain part I geologic evolution. In: Decker, R.W., Wright, T.L., Stauffer, P.H. (Eds.), Volcanism in Hawaii: Papers to commemorate the 75th anniversary of the founding of the Hawaiian Volcano Observatory, pp. 5–54 Geol. Soc. Prof. Pap. Vol. 1350, U. S. Geological Survey.
Clague, D.A., Frey, F.A., 1982. Honolulu Volcanics, Oahu: implications for the oceanic mantle below Hawaii. J. Petrol. 23 (3), 447–504.
Clague, D.A., Sherrod, D.R., 2014. Growth and degradation of Hawaiian volcanoes. In: Poland, M.P., Takahashi, T.J., Landowski, C.M. (Eds.), Characteristic of Hawaiian Volcanoes, pp. 97–146 U.S. Geol. Sur. Prof. Pap. 1801.
Clague, D.A., Dalrymple, G.B., Moberly, R., 1975. Petrography and K-Ar ages of dredged volcanic rocks from the Western Hawaiian Ridge and the Southern Emperor Seamount chain. Geol. Soc. Am. Bull. 86, 991–998.
Clague, D.A., Frey, F.A., Garcia, M.O., Huang, S., McWilliams, M., Beeson, M.H., 2016. Compositional heterogeneity of the Sugarloaf melilite nephelinite flow, Honolulu Volcanics, Hawai'i. Geochim. Cosmochim. Acta 185, 251–277.
Coffin, M.F., Pringle, M.S., Duncan, R.A., Gladszenko, T.P., Storey, M., Müller, R.D., Gahagan, L.A., 2002. Kerguelen hotspot magma output since 130 Ma. J. Petrol. 43 (7), 1121–1137.
Cottrell, R.D., Tarduno, J.A., 2003. A Late Cretaceous pole for the Pacific plate: implications for apparent and true polar wander and the drift of hotspots. Tectonophys 362, 321–333.
Courtillot, V., Davaille, A., Besse, J., Stock, J., 2003. Three distinct types of hotspots in the Earth's mantle. Earth Planet. Sci. Lett. 205, 295–308.
Cousens, B.L., Clague, D.A., 2015. Shield to rejuvenated stage volcanism on Kauai and Niihau, Hawaiian Islands. J. Petrol. 56 (8), 1547–1584.
Cousens, B.L., Spera, F.J., Tilton, G.R., 1990. Isotopic patterns in silicic ignimbrites and lava flows of the Mogan and lower Fataga Formations, Gran Canaria, Canary Islands: temporal changes in mantle source composition. Earth Planet. Sci. Lett. 96, 319–335.
Cousens, B.L., Spera, F.J., Dobson, P.F., 1993. Post-eruptive alteration of silicic ignimbrites and lavas, Gran Canaria, Canary Islands: Strontium, neodymium, lead, and oxygen isotopic evidence. Geochim. Cosmochim. Acta 57, 631–640.
Cousens, B.L., Clague, D.A., Sharp, W.D., 2003. Chronology, chemistry, and origin of trachytes from Hualalai Volcano, Hawaii. Geochem. Geophys. Geosyst. 4 (9), 1078–1105.
Dalrymple, G.B., Clague, D.A., 1976. Age of the Hawaiian-Emperor bend. Earth Planet. Sci. Lett. 31, 313–329.
Dalton, C.A., Langmuit, C.H., Gale, A., 2014. Geophysical and geochemical evidence for deep temperature variations beneath mid-ocean ridges. Science 344, 80–83.
Davies, D.R., Davies, J.H., 2009. Thermally-driven mantle plumes reconcile multiple hotspot observations. Earth Planet. Sci. Lett. 278, 50–54.
DeFelice, C., Mallick, S., Saal, A.E., Huang, S., 2019. An isotopically depleted lower mantle component is intrinsic to the Hawaiian mantle plume. Nat. Geosci. 12, 487–492.
Dixon, J., Clague, D.A., Cousens, B., Monsalve, M.L., Uhl, J., 2008. Carbonatite and silicate melt metasomatism of the mantle surrounding the Hawaiian plume: evidence from volatiles, trace elements, and radiogenic isotopes in rejuvenated-stage lavas from Niihau, Hawaii. Geochem. Geophys. Geosyst. 9 (9), Q09005.
Doin, M.P., Fleitout, L., 1996. Thermal evolution of the oceanic lithosphere: an alternative view. Earth Planet. Sci. Lett. 142, 121–136.
Duncan, R.A., Clague, D.A., 1984. The earliest volcanism on the Hawaiian Ridge. EOS Transaction, American Geophysical Union 65, 1076.
Duncan, R.A., Fisk, M.R., White, W.M., Nielsen, R.L., 1994. Tahiti: geochemical evolution of a French Polynesian volcano. J. Geophys. Res. 99 (B12), 24341–24357.
Dyment, J., 1998. Evolution of the Carlsberg Ridge between 60 and 45 Ma: Ridge propagation, spreading asymmetry, and the Deccan-Reunion hotspot. J. Geophys. Res. 103 (B10), 24067–24084.
Farnetani, D.G., Richards, M.A., 1995. Thermal entrainment and melting in mantle plumes. Earth Planet. Sci. Lett. 136, 251–267.
Feigenson, M.D., 1984. Geochemistry of Kauai volcanics and a mixing model for the origin of Hawaiian alkali basalts. Contrib. Min. Petrol. 87, 109–119.
Feigenson, M.D., Hofmann, A.W., Spera, F.J., 1983. Case studies on the origin of basalt II. The transition from tholeiitic to alkalic volcanism on Kohala volcano, Hawaii. Contrib. Min. Petrol. 84, 390–405.
Fekiacova, Z., Abouchami, W., Galer, S.J.G., Garcia, M.O., Hofmann, A.W., 2007. Origin and temporal evolution of Ko'olau Volcano, Hawai'i: Inferences from isotope data on the Ko'olau scientific drilling project (KSDP), the Honolulu volcanics and ODP Site 843. Earth Planet. Sci. Lett. 261, 65–83.
Fitton, J.G., Saunders, A.D., Norry, M.J., Hardarson, B.S., Taylor, R.N., 1997. Thermal and chemical structure of the Iceland plume. Earth Planet. Sci. Lett. 153, 197–208.
Fourny, A., Weis, D., Scoates, J.S., 2016. Comprehensive Pb-Sr-Nd-Hf isotopic, trace

element, and mineralogical characterization of mafic to ultramafic rock reference materials. Geochem. Geophys. Geosyst. 17 (3), 739–773.
French, S.W., Romanowicz, B., 2015. Broad plumes rooted at the base of the Earth's mantle beneath major hotspots. Nature 525, 95–99.
Frey, F.A., Rhodes, J.M., 1993. Intershield geochemical differences among Hawaiian volcanoes: implications for source compositions, melting process, and magma ascent paths. Philosophical Trans. Royal Soc. Lond. 342, 121–136.
Frey, F.A., Wise, W.S., Garcia, M.O., West, H., Kwon, S.-T., Kennedy, A., 1990. Evolution of Mauna Kea volcano, Hawaii: petrologic and geochemical constraints on postshield volcanism. J. Geophys. Res. 95 (B2), 1271–1300.
Frey, F.A., Garcia, M.O., Roden, M.F., 1994. Geochemical characteristics of Koolau volcano: implications of intershield geochemical differences among Hawaiian volcanoes. Geochim. Cosmochim. Acta 58 (5), 1441–1462.
Frey, F.A., Clague, D., Mahoney, J.J., Sinton, J.M., 2000. Volcanism at the edge of the Hawaiian Plume: petrogenesis of submarine alkalic lavas from the North Arch Volcanic Field. J. Petrol. 41 (5), 667–691.
Frey, F.A., Huang, S., Blichert-Toft, J., Regelous, M., Boyet, M., 2005. Origin of depleted components in basalt related to the Hawaiian hot spot: evidence from isotopic and incompatible element ratios. Geochem. Geophys. Geosyst. 6, Q02L07.
Frey, F.A., Huang, S., Xu, G., Jochum, K.P., 2016. The geochemical components that distinguish Loa- and Kea-trend Hawaiian shield lavas. Geochim. Cosmochim. Acta 185, 160–181.
Gale, A., Dalton, C.A., Langmuir, C.H., Su, Y., Schilling, J.-G., 2013. The mean composition of ocean ridge basalts. Geochem. Geophys. Geosyst. 14 (3), 486–518.
Garcia, M.O., Grooms, D.G., Naughton, J.J., 1987. Petrology and geochronology of volcanic rocks from seamounts along and near the Hawaiian Ridge: Implications for propagation rate of the ridge. Lithos 20, 323–336.
Garcia, M.O., Ito, G., Weis, D., Geist, D., Swinnard, L., Bianco, T., Flinders, A., Taylor, B., Appelgate, B., Blay, C., Hanano, D., Nobre Silva, I., Naumann, T., Maerschalk, C., Harpp, K., Christensen, B., Sciaroni, L., Tagami, T., Yamasaki, S., 2008. Widespread secondary volcanism near Northern Hawaiian Islands. EOS 89 (52), 542–543.
Garcia, M.O., Swinnard, L., Weis, D., Greene, A.R., Tagami, T., Sano, H., Gandy, C.E., 2010. Petrology, geochemistry, and geochronology of Kaua'i lavas over 4.5 Myr: implications for the origin of rejuvenated volcanism and the evolution of the Hawaiian Plume. J. Petrol. 51, 1507–1540.
Garcia, M.O., Smith, J.R., Tree, J.P., Weis, D., Harrison, L., Jicha, B.R., 2015. Petrology, geochemistry, and ages of lavas from the Northwest Hawaiian Ridge volcanoes. In: In: Neal, C.R., Sager, W.W., Sano, T., Erba, E. (Eds.), The Origin, Evolution, and Environmental Impact of Oceanic Large Igneous Provinces 511. Geological Society of America, Inc., pp. 1–26 Geol. Soc. Sp. Pap.
Garcia, M.O., Weis, D., Jicha, B.R., Ito, G., Hanano, D., 2016. Petrology and geochronology of lavas from Ka'ula Volcano: Implications for rejuvenated volcanism of the Hawiian mantle plume. Geochim. Cosmochim. Acta 185, 278–301.
Garnero, E.J., McNamara, A.K., Shim, S.-H., 2016. Continent-sized anomalous zones with low seismic velocity at the base of the Earth's mantle. Nat. Geosci. 9, 481–489.
Geldmacher, J., Höfig, T.W., Hauff, F., Hoernle, K., Garbe-Schuönberg, D., Wilson, D.S., 2013. Influence of the Galápagos hotspot on the East Pacific Rise during Miocene superfast spreading. Geology 41 (2), 183–186.
Genske, F., Stracke, A., Berndt, J., Klemme, S., 2019. Process-related isotope variability in oceanic basalts revealted by high-precision Sr isotope ratios in olivine-hosted melt inclusions. Chem. Geol. 524, 1–10.
Greene, A., Garcia, M.O., Weis, D., Ito, G., Kuga, M., Robinson, J., Yamasaki, S., 2010. Low-productivity Hawaiian volcanism between Kaua'i and O'ahu. Geochem. Geophys. Geosyst. 11, Q0AC08.
Haase, K.M., Beier, C., Kemner, F., 2019. A comparison of the magmatic evolution of Pacific intraplate volcanoes: constraints on melting in mantle plumes. Front. Earth Sci. 6, 242.
Hanan, B.B., Graham, D.W., 1996. Lead and helium isotope evidence from oceanic basalts for a common deep source of mantle plumes. Science 272, 991–995.
Hanano, D., Scoates, J.S., Weis, D., 2009. Alteration mineralogy and the effect of acid-leaching on the Pb-isotope systematics of ocean-island basalts. Am. Min. 94, 17–26.
Hanano, D., Weis, D., Scoates, J.S., Aciego, S., De Paolo, D.J., 2010. Horizontal and vertical zoning of heterogeneities in the Hawaiian mantle plume from the geochemistry of consecutive postshield volcano pairs: Kohala-Mahukona and Mauna Kea–Hualalai. Geochem. Geophys. Geosyst. 11, Q01004.
Harpp, K.S., Wirth, K.R., Teasdale, R., Blair, S., Reed, L., Barr, J., Pistiner, J., Korich, D., 2014. Plume-ridge interaction in the Galápagos: Perspectives from Wolf, Darwin, and Genovesa Islands. In: In: Harpp, K.S., Mittelstaedt, E., d'Ozouville, Noémi, Graham, D.W. (Eds.), The Galápagos: A natural laboratory for the earth sciences Vol. 204. American Geophysical Union, pp. 448 Geophys. Monogr. Ser.
Harrison, L.N., Weis, D., 2018. The size and emergence of geochemical heterogeneities in the Hawaiian mantle plume constrained by Sr-Nd-Hf isotopic variations over ~47 million years. Geochem. Geophys. Geosyst. 19, 2823–2842.
Harrison, L.N., Weis, D., Garcia, M.O., 2017. The link between Hawaiian mantle plume composition, magmatic flux, and deep mantle geodynamics. Earth Planet. Sci. Lett. 463, 298–309.
Hart, S.R., Erlank, A.J., Kable, E.J.D., 1974. Sea floor basalt alteration: some chemical and Sr isotopic effects. Contrib. Min. Petrol. 44, 219–230.
Hassan, R., Flament, N., Gurnis, M., Bower, D.J., Müller, D., 2015. Provenance of plumes in global convection models. Geochem. Geophys. Geosyst. 16, 1465–1489.
Hassan, R., Müller, R.D., Gurnis, M., Williams, S.E., Flament, N., 2016. A rapid burst in hotspot motion through the interaction of tectonics and deep mantle flow. Nature 533, 239–242.
Hauri, E.H., Hart, S.R., 1993. Re-Os isotope systematics of HIMU and EMII oceanic island basalts from the South Pacific Ocean. Earth Planet. Sci. Lett. 114, 353–371.
Hawkins, J.W., Natland, J.H., 1975. Nephelinites and basanites of the Samoan linear volcanic chain: their possible tectonic significance. Earth Planet. Sci. Lett. 24, 427–439.
Heydolph, K., Murphy, D.T., Geldmacher, J., Romanova, I.V., Greene, A., Hoernle, K., Weis, D., Mahoney, J., 2014. Plume versus plate origin for the Shatsky Rise oceanic plateau (NW Pacific): insights from Nd, Pb, and Hf isotopes. Lithos 200–201, 49–63.
Hildenbrand, A., Gillot, P.-Y., Le Roy, I., 2004. Volcano-tectonic and geochemical evolution of an oceanic intra-plate volcano: Tahiti-Nui (French Polynesia). Earth Planet. Sci. Lett. 217, 349–365.
Hoernle, K., Schminke, H.-U., 1993. The petrology of the tholeiites through melilite nephlinites on Gran Canaria, Canary Islands: crystal fractionation, accumulation, and depths of melting. J. Petrol. 34 (3), 573–597.
Hoernle, K., Rohde, J., Hauff, F., Garbe-Schonberg, D., Homrighausen, S., Werner, R., Morgan, J.P., 2015. How and when plume zonation appeared during the 132 Myr evolution of the Tristian Hotspot. Nat. Comm. 6 10 p.
Hofmann, A.W., 2014. Sampling mantle heterogeneity through oceanic basalts: Isotopes and trace elements. In: second edition. In: Holland, H.D., Turekian, K.K. (Eds.), Treatise of Geochem Vol 3. pp. 67–101.
Hofmann, A.W., Farnetani, C.G., 2013. Two views of Hawaiian plume structure. Geochem. Geophys. Geosyst. 14, 5308–5322.
Holcomb, R.T., Robinson, J.E., 2004. Maps of Hawaiian Islands Exclusive Economic Zone interpreted from GLORIA sidescan-sonar imagery. U.S. Geol. Surv. Sci. Investig Map 2824.
Huang, S., Frey, F.A., 2005. Recycled oceanic crust in the Hawaiian Plume: evidence from temporal geochemical variations within the Koolau Shield. Contrib. Min. Petrol. 149, 556–575.
Huang, S., Regelous, M., Thordarson, T., Frey, F.A., 2005a. Petrogenesis of lavas from Detroit Seamount: geochemical differences between Emperor Chain and Hawaiian volcanoes. Geochem. Geophys. Geosyst. 6, Q01L06.
Huang, S., Frey, F.A., Blichert-Toft, J., Rodor, R.V., Bauer, G.R., Xu, G., 2005b. Enriched components in the Hawaiian plume: evidence from Kahoolawe Volcano, Hawaii. Geochem. Geophys. Geosyst. 6 (11), Q11006.
Huang, S., Hall, P.S., Jackson, M.G., 2011. Geochemical zoning of volcanic chains associated with Pacific hotspots. Nat. Geosci. 4, 874–878.
Humphris, S.E., Thompson, G., 1978. Hydrothermal alteration of oceanic basalts by seawater. Geochim. Cosmochim. Acta 42, 107–125.
Ito, G., Clift, P.D., 1998. Subsidence and growth of Pacific Cretaceous plateaus. Earth Planet. Sci. Lett. 161, 85–100.
Ito, G., Lin, J., Graham, D., 2003. Observational and theoretical studies of the dynamics of mantle plume-mid-ocean ridge interaction. Rev. Geophys 41, 4/1017.
Jackson, M.G., Konter, J.G., Becker, T.W., 2017. Primordial helium entrained by the hottest mantle plumes. Nature 542, 340–343. https://doi.org/10.1038/nature21023.
Jackson, E.D., Silver, E.L.I.A., Dalrymple, G.B., 1972. Hawaiian-Emperor chain and its relation to Cenozoic circum-pacific tectonics. Bull. Geol. Soc. Am. 83 (3), 601.
Jackson, M.J., Weis, D., Huang, S., 2012. Major element variations in Hawaiian shield lavas: source features and perspectives from global ocean island basalt (OIB) systematics. Geochem. Geophys. Geosyst. 13 (9), Q09009.
Jackson, M.G., Hart, S.R., Konter, J.G., Kurz, M.D., Blusztajn, J., Farley, K.A., 2014. Helium and lead isotopes reveal the geochemical geometry of the Samoan plume. Nature 514, 355–358.
Jacobsen, S.B., Wasserburg, G.J., 1980. Sm–Nd evolution of chondrites. Earth Planet. Sci. Lett. 50, 139–155.
Janney, P.E., Castillo, P.R., 1997. Geochemistry of Mesozoic Pacific mid-ocean ridge basalt: constraints on melt generation and the evolution of the Pacific upper mantle. J. Geophys. Res. 102 (B3), 5207–5229.
Jellinek, M., Manga, M., 2004. Links between long-lived hot spots, mantle plumes, D", and plate tectonics. Rev. Geophys. 42, RG3002.
Jicha, B.R., Garcia, M.O., Wessel, P., 2018. Mid-Cenozoic Pacific plate motion change: implications for the Northwest Hawaiian Ridge and circum-Pacific. Geology 46, 939–942.
Johansen, T.S., Hauff, F., Hoernle, K.A., Klügel, A., Kokfelt, T.F., 2005. Basanite to phonolite differentiation within 1550-1750 yr: U-Th-Ra isotopic evidence from the a.d. 1585 eruption on La Palma, Canary Islands. Geology 33, 897–900.
Jones, R.E., van Keken, P.E., Hauri, E.H., Tucker, J.M., Vervoort, J., Ballentine, C.J., 2019. Origins of the terrestrial Hf-Nd mantle array: evidence from a combined geodynamical-geochemical approach. Earth Planet. Sci. Lett. 518, 26–39.
Keller, R.A., Duncan, R.A., Fisk, M.R., 1995. Geochemistry and $^{40}Ar/^{39}Ar$ geochronology of basalts from ODP Leg 145 (North Pacific transect). In: In: Rea, D.K., Basov, I.A., Scholl, D.W., Allan, J.F. (Eds.), Proceed. Ocean Drill. Prog. Sci. Res. Vol. 145. pp. 333–344.
Keller, R.A., Fisk, M., White, W.M., 2000. Isotopic evidence for Late Cretaceous plume-ridge interaction at the Hawaiian hotspot. Nature 405, 673–676.
Keller, R.A., Graham, D.W., Farlay, K.A., Duncan, R.A., Lupton, J.E., 2004. Cretaceous-to-recent record of elevated $^{3}He/^{4}He$ along the Hawaiian-Emperor volcanic chain. Geochem. Geophys. Geosyst. 5 (12), Q12L05.
Kerr, B.C., Scholl, D.W., Klemperer, S.L., 2005. Seismic stratigraphy of Detroit Seamount, Hawaiian-Emperor Seamount chain: Post-hot-spot shield-building volcanism and deposition of the Meiji drift. Geochem. Geophys. Geosyst. 6 (7), Q07L10.
Kingsley, R.H., Schilling, J.-G., 1998. Plume-ridge interaction in the Easter-Salas y Gomez seamount chain-Easter microplate system: Pb isotope evidence. J. Geophys. Res. 103 (B10), 24159–24177.
Kingsley, R.H., Blichert-Toft, J., Fontignie, D., Schilling, J.-G., 2007. Hafnium, neodymium, and strontium isotope and parent-daughter element systematics in basalts from the plume-ridge interaction system of the Salas y Gomez seamount chain and Easter Microplate. Geochem. Geophys. Geosyst. 8 (4), Q04005.
Konrad, K., Koppers, A.A.P., Steinberger, B., Finlayson, V.A., Konter, J.G., Jackson, M.G., 2018. On the relative motions of long-lived Pacific mantle plumes. Nat. Comm. 9,

854.
Konter, J.G., Jackson, M.G., 2012. Large volumes of rejuvenated volcanism in Samoa: Evidence supporting tectonic influence on late-stage volcanism. Geochem. Geophys. Geosyst. 13 (1), Q0AM04.
Kopp, H., Kopp, C., Morgan, J.P., Flueh, E.R., Weinrebe, W., 2003. Fossil hot spot-ridge interaction in the Musicians seamount Province: geophysical investigations of hot spot volcanism at volcanic elongated ridges. J. Geophys. Res. 108 (B3), 2160–2180.
Koppers, A.A.P., Staudigel, H., Pringle, M.S., Wijbrans, J.R., 2003. Short-lived and discontinuous intraplate volcanism in the South Pacific: hot spots or extensional volcanism? Geochem. Geophys. Geosyst. 4 (10), 1089.
Koppers, A.A.P., Duncan, R.A., Steinberger, B., 2004. Implications of a nonlinear 40Ar/39Ar age progression along the Louisville seamount trail for models of fixed and moving hot spots. Geochem. Geophys. Geosyst. 5 (6), Q06L02.
Lanphere, M.A., Dalrymple, G.B., Clague, D.A., et al., 1980. Rb-Sr systematics of basalts from the Hawaiian-Emperor volcanic chain. In: Jackson, E.D. (Ed.), Initial reports of the deep sea drilling project, pp. 695–706 Deep Sea Drilling Project 55.
Larson, R.L., 1991. Geological consequences of superplumes. Geology 19, 963–966.
Lassiter, J.C., Hauri, E., 1998. Osmium-isotope variations in Hawaiian lavas: evidence for recycled oceanic lithosphere in the Hawaiian plume. Earth Planet. Sci. Lett. 164, 483–496.
Lassiter, J.C., Hauri, E.H., Reiners, P.W., Garcia, M.O., 2000. Generation of Hawaiian post-erosional lavas by melting of a mixed lherzolite/pyroxenite source. Earth Planet. Sci. Lett. 178, 269–284.
Le Saout, M., Deschamps, A., Soule, S.A., Gente, P., 2014. Segmentation and eruptive activity along the East Pacific Rise at 16°N, in relation with the nearby Mathematician hotspot. Geochem. Geophys. Geosyst. 15, 4380–4399.
Leahy, G.M., Collins, J.A., Wolfe, C.J., Laske, G., Solomon, S.C., 2010. Underplating of the Hawaiian Swell: evidence from teleseismic receiver functions. Geophys. J. Intern. 183, 313–329.
Li, X., Kind, R., Yuan, X., Wölbern, I., Hanka, W., 2004. Rejuvenation of the lithosphere by the Hawaiian plume. Nature 427, 827–829.
Liu, C.-Z., Snow, J.E., Hellebrand, E., Brügmann, G., von der Handt, A., Büchl, A., Hofmann, A.W., 2008. Ancient, highly heterogeneous mantle beneath Gakkel ridge, Arctic Ocean. Nature 452, 311–316.
Lonsdale, P., 1988. Paleogene history of the Kula plate: offshore evidence and onshore implications. GSA Bull. 100 (5), 733–754.
Lonsdale, P., Dieu, J., Natland, J., 1993. Posterosional volcanism in the Cretaceous part of the Hawaiian hotspot trail. J. Geophys. Res. 98 (B3), 4081–4098.
Luo, J., Kong, X., 2006. Half-life of ^{176}Lu. App. Rad. Isotopes 64 (5), 588–590.
Macdonald, G.A., Katsura, T., 1964. Chemical composition of the Hawaiian lavas. J. Petrol. 5, 82–133.
MacLeod, S.J., Williams, S.E., Mathews, K.J., Muller, R.D., Qin, X., 2017. A global review and digital database of large-scale extinct spreading centers. Geosphere 13 (3), 911–949.
Malaviarachchi, S.P.K., Makishima, A., Tanimoto, M., Kuritani, T., Nakamura, E., 2008. Highly unradiogenic lead isotope ratios from the Horoman peridotitie in Japan. Nat. Geosci. 1, 859–863.
Mallick, S., Salters, V.J.M., Langmuir, C.H., 2019. Geochemical variability along the Northeran East Pacific Rise: coincident source composition and ridge segmentation. Geochem. Geophys. Geosyst. 20, 1889–1911.
Mammerickx, J., Sharman, G.F., 1988. Tectonic evolution of the North Pacific during the Cretaceous quiet period. Journal of Geophysical Research 93 (B4), 3009–3024.
McDonough, W.F., Sun, S.-S., 1995. The composition of the Earth. Chem. Geol. 120, 223–253.
Mittelstaedt, E., Ito, G., 2005. Plume-ridge interaction, lithospheric stresses, and the origin of near-ridge volcanic lineaments. Geochem. Geophys. Geosyst. 6 (6), Q06002.
Miyazaki, T., Kimura, J.-I., Senda, R., Vaglarov, B.S., Chang, Q., Takahashi, T., Hirahara, Y., Hauff, F., Hayasaka, Y., Sano, S., Shimoda, G., Ishizuka, O., Kawabata, H., Hirano, N., Machida, S., Ishii, T., Tani, K., Yoshida, T., 2015. Missing western half of the Pacific Plate: geochemical nature of the Izanagi-Pacific Ridge interaction with a stationary boundary between the Indian and Pacific mantles. Geochem. Geophys. Geosyst. 16, 3309–3332.
Montelli, R., Nolet, G., Dahlen, F.A., Masters, G., 2006. A catalogue of deep mantle plumes: new results from finite frequency tomography. Geochem. Geophys. Geosyst. 7, Q11007.
Moore, J., White, W.M., Paul, D., Duncan, R.A., Abouchami, W., Galer, S.J.G., 2011. Evolution of shield-building and rejuvenescent volcanism of Mauritius. Journal of Volcanol. Geotherm. Res. 207, 47–66.
Mougel, B., Agranier, A., Hemond, C., Gente, P., 2014. A highly unradiogenic lead isotopic signature revealed by volcanic rocks from the East Pacific Rise. Nat. Comm. 5, 4474.
Mougel, B., Moreira, M., Agranier, A., 2015. A "high ^{4}He/^{3}He" mantle material detected under the East Pacific Rise (15°4′N). Geophys. Res. Lett. 42, 1375–1383.
Mukhopadhyay, S., Lassiter, J.C., Farley, K.A., Bogue, S.W., 2003. Geochemistry of Kauai shield-stage lavas: Implications for the chemical evolution of the Hawaiian plume. Geochem. Geophys. Geosyst. 4, 1008.
Müller, R.D., Seton, M., Zahirovic, S., Williams, S.E., Matthews, K.J., Wright, N.M., Shephard, G.E., Maloney, K.T., Barnett-Moore, N., Hosseinpour, M., Bower, D.J., Cannon, J., 2016. Ocean basin evolution and global-scale plate reorganization events since Pangea breakup. J. Annu. Rev. Earth Planet. Sci. 44, 107–138.
Murton, B.J., Taylor, R.N., Thirlwall, M.F., 2002. Plume-ridge interaction: A geochemical perspective from the Reykjanes Ridge. J. Petrol. 43 (11), 1987–2012.
Natland, J.H., 1980. The progression of volcanism in the Samoan linear volcanic chain. Am. J. Sci. 280A, 709–735.
Neave, D.A., Namur, O., Shorttle, O., Holtz, F., 2019. Magmatic evolution biases basaltic records of mantle chemistry towards melts from recycled sources. Earth Planet. Sci. Lett. 520, 199–211.
Nobre Silva, I.G., Weis, D., Barling, J., Scoates, J.S., 2009. Leaching systematics and matrix elimination for the determination of high-precision Pb isotope compositions of ocean island basalts Geochem. Geophys. Geosyst.10, Q08012.
Nobre Silva, I.G., Weis, D., Scoates, J.S., 2013a. Isotopic systematics of the early Mauna Kea shield phase and insight into the deep mantle beneath the Pacific Ocean. Geochem. Geophys. Geosyst. 14 (3), 659–676.
Nobre Silva, I.G., Weis, D., Scoates, J.S., 2013b. The Ninetyeast Ridge and its relation to the Kerguelen, Amsterdam, and St. Paul hotspots in the Indian Ocean. J. Petrol. 54, 1177–1210.
Norton, I.O., 2007. Speculations on Cretaceous tectonic history of the northwest Pacific and a tectonic origin for the Hawaii hotspot. In: Foulger, G.R., Jurdy, D.M. (Eds.), Plates, plumes and planetary processes, pp. 451–470 Geol. Soc. Am. Sp. Pap. 430.
O'Connor, J.M., Steinberger, B., Regelous, M., Koppers, A., Wijbrans, J., Stoffers, P., Jokat, W., Garbe-Schonberg, D., 2013. Constraints on past plate and mantle motion from new ages for the Hawaiian-Emperor seamount chain. Geochem. Geophys. Geosyst. 14, 4564–4584.
O'Nions, R.K., McKenzie, D., 1993. Estimates of mantle thorium/uranium ratios from the Th, U, and Pb isotope abundances in basaltic melts. Phil. Trans. R. Soc. A. 342, 65–77.
Parai, R., Mukhopadhyay, S., Standish, J.J., 2012. Heterogeneous upper mantle Ne, Ar, and Xe isotopic characterics and a possible Dupal noble gas signature recorded from the Southwest Indian Ridge. Earth Planet. Sci. Lett. 359-360, 227–239.
Paris, R., Guillou, H., Carracedo, J.C., Perez Torrado, F.J., 2005. Volcanic and morphological evolution of La Gomera (Canary Islands), based on new K-Ar ages and magnetic stratigraphy: implications for oceanic island evolution. J. Geol. Soc. Lond. 162, 501–512.
Paul, D., White, W.M., Blichert-Toft, J., 2005. Geochemistry of Mauritius and the origin of rejuvenescent volcanism on oceanic island volcanoes. Geochem. Geophys. Geosyst. 6 (6), Q06007.
Pearce, J.A., 2008. Geochemical fingerprinting of oceanic basalts with applications to ophiolite classification and the search for Archean oceanic crust. Lithos 100, 14–48.
Pietruszka, A.J., Norman, M.D., Garcia, M.O., Marske, J.P., Burns, D.H., 2013. Chemical heterogeneity in the Hawaiian mantle plume from the alteration and dehydration of recycled oceanic crust. Earth Planet. Sci. Lett. 361, 298–309.
Portnyagin, M., Davelyev, D., Hoernle, K., Hauff, F., Garbe-Schonberg, D., 2008. Mid-Cretaceous Hawaiian tholeiites preserved in Kamchatka. Geology 36 (11), 903–906.
Putirka, K., 2005. Mantle potential temperatures at Hawaii, Iceland, and the mid-ocean ridge system, as inferred from olivine phenocrysts: Evidence for thermally driven mantle plumes. Geochem. Geophys. Geosyst. 6 (5), Q05L08.
Regelous, M., Hofmann, A.W., Abouchami, W., Galer, S.J.G., 2003. Geochemistry of lavas from the Emperor Seamounts and the geochemical evolution of Hawaiian magmatism from 85 to 42 Ma. J. Petrol. 44, 113–140.
Reiners, P.W., Nelson, B.K., 1998. Temporal-compositional-isotopic trends in rejuvenated-stage magmas of Kauai, Hawaii, and implications for mantle melting processes. Geochim. Cosmochim. Acta 62 (13), 2347–2368.
Reinhard, A.A., Jackson, M.G., Blusztajn, J., Koppers, A.A.P., Simms, A.R., Konter, J.G., 2019. "Petit spot" rejuvenated volcanism superimposed on plume-derived Samoan shield volcanoes: evidence from a 645-m drill core from Tutuila Island, American Samoa. Geochem. Geophys. Geosys. 20, 1485–1507.
Rhodes, J.M., Vollinger, M.J., 2004. Composition of basaltic lavas sampled by phase-2 of the Hawaii Scientific Drilling Project: geochemical stratigraphy and magma types. Geochem. Geophys. Geosyst. 5, Q03G13.
Ribe, N.M., Christensen, U.R., 1999. The dynamical origin of Hawaiian volcanism. Earth Planet. Sci. Lett. 171, 517–531.
Roden, M.F., Frey, F.A., Clague, D.A., 1984. Geochemistry of tholeiitic and alkalic lavas from the Koolau Range, Oahu, Hawaii: implications for Hawaiian volcanism. Geochim. Cosmochim. Acta 58, 1437–1446.
Roden, M.F., Trull, T., Hart, S.R., Frey, F.A., 1994. New He, Nd, Pb, and Sr isotopic constraints on the constitution of the Hawaiian plume: results from Koolau Voclano, Oahu, Hawaii, USA. Geochim. Cosmochim. Acta 58 (5), 1431–1440.
Rodriguez-Gonzalez, A., Perez-Torrado, F.J., Fernandez-Tuiel, J.L., Aulinas, M., Paris, R., Moreno-Medina, C., 2018. The Holocene volcanism of Gran Canaria (Canary Islands, Spain). J. Maps 14 (2), 620–629.
Rudge, J.F., Maclennan, J., Stracke, A., 2013. The geochemical consequences of mixing melts from a heterogeneous mantle. Geochim. Cosmochim. Acta 114, 112–143.
Salters, V.J.M., Blichert-Toft, J., Fekiacova, Z., Sachi-Kocher, A., Bizimis, M., 2006. Isotope and trace element evidence for depleted lithosphere in the source of enriched Ko'olau basalts. Contrib. Mineral. Petrol. 151, 297–312.
Salters, V.J.M., Mallick, S., Hart, S.R., Langmuir, C.E., Stracke, A., 2011. Domains of depleted mantle: new evidence from hafnium and neodymium isotopes. Geochem. Geophys. Geosyst. 12 (8), Q08001.
Sanfilippo, A., Salters, V., Tribuzio, R., Zanetti, A., 2019. Role of ancient, ultra-depleted mantle in Mid-Ocean-Ridge magmatism. Earth. Planet. Sci. Lett. 511, 89–98.
Sano, S., Hayasaka, Y., 2004. Sr and Nd isotope geochemistry of Hole 1179D basalts. In: In: Sager, W.W., Kanazawa, T., Escutia, C. (Eds.), In Proceed. Ocean Drill. Prog. Sci. Results 191. pp. 1–11.
Schilling, J.-G., 1991. Fluxes and excess temperatures of mantle plumes inferred from their interaction with migrating mid-ocean ridges. Nature 352, 397–403.
Schilling, J.-G., Zajac, M., Evans, R., Johnston, T., White, W., Devine, J.D., Kingsley, R., 1983. Petrologic and geochemical variations along the Mid-Atlantic ridge from 29°N to 73°N. Am. J. Sci. 283, 510–586.
Schudel, G., Lai, V., Gordon, K., Weis, D., 2015. Trace element characterization of USGS reference materials by HR-ICP-MS and Q-ICP-MS. Chem. Geol. 410, 223–236.
Shafer, J.T., Neal, C.R., Regelous, M., 2005. Petrogenesis of Hawaiian postshield lavas: evidence from Nintoku Seamount, Emperor Seamount chain. Geochem. Geophys. Geosyst. 6, Q05L09.

Sharp, W.D., Clague, D.A., 2006a. 50-Ma initiation of the Hawaiian-Emperor bend records major change in Pacific Plate motion. Science 313, 1281–1284.
Sharp, W.D., Clague, D., 2006b. A. 50-Ma initiation of Hawaiian-Emperor bend records major change in Pacific plate motion. Science 313, 1281–1284.
Sherrod, D.R., Sinton, J.M., Watkins, S.E., Brunt, K.M., 2007. Geologic map of the state of Hawai'i. U.S. Geol. Surv. Rep. 2007-1089, 1–83.
Sleep, N.H., 1990. Hotspots and mantle plumes: some phenomenology. J. Geophys. Res. 95 (B5), 6715–6736.
Sleep, N.H., 2007. Weak thermal convection within tilted plume conduits. Geochem. Geophys. Geosyst. 8 (11), Q11005.
Sleep, N.H., 2011. Small-scale convection beneath oceans and continents. Chinese Sci. Bull. 56 (13), 1292–1317.
Small, C., 1995. Observations of ridge-hotspot interactions in the Southern Ocean. J. Geophys. Res. 100 (B9), 17931–17946.
Smith, J.R., Boston, B., Dechnik, B., Habel, S., Harrison, L., Kelley, C., Leonard, J., Lichowski, F., Luers, D., Miller, J., Orange, R., Patterson, M., Shiro, B., Taylor, J., Togia, H., Tree, J., Tucker, J., Wagner, D., Webster, J., Wright, N., 2014. An introduction to new multibeam data from the Papahanaumokuakea Marine National Monument in the Northwestern Hawaiian Islands Obtained by the R/V Falkor. Am. Geophys. Un. Abst., OS34A-06.
Sobolev, A.V., Hofmann, A.W., Sobolev, S.V., Nikogosian, I.K., 2005. An olivine-free mantle source of Hawaiian shield basalts. Nature 434, 590–597.
Stearns, H.T., 1946. Geology of the Hawaiian Islands: Hawaii (Terr.) Division of Hydrography Bulletin 8. 106 p.. .
Steinberger, B., 2000. Plumes in a convecting mantle: Models and observations for individual hotspots. Journal of Geophysical Research 105, 127–152.
Steinberger, B., Sutherland, R., O'Connell, R.J., 2004. Prediction of Emperor-Hawaii seamount locations from a revised model of global plate motion and mantle flow. Nature 430, 167–173.
Stracke, A., 2012. Earth's heterogeneous mantle: A product of convection-driven interaction between crust and mantle. Chem. Geol. 331, 274–299.
Stracke, A., Salters, V.J.M., Sims, K.W.W., 1999. Assessing the presence of garnet-pyroxenite in the mantle sources of basalts through combined hafnium-neodymium-thorium isotope systematics. Geochem. Geophys. Geosyst. 1 (1), 1006.
Stracke, A., Hofmann, A.W., Hart, S.R., 2005. FOZO, HIMU, and the rest of the mantle zoo. Geochem. Geophys. Geosyst. 6 (5), Q05007.
Stracke, A., Snow, J.E., Hellebrand, E., von der Handt, A., Bourdon, B., Birbaum, K., Günther, D., 2011. Abyssal peridotite Hf isotopes identify extreme mantle depletion. Earth Planet. Sci. Lett. 308, 359–368.
Stracke, A., Genske, F., Berndt, J., Koornneef, J.M., 2019. Ubiquitious ultra-depleted domains in Earth's mantle. Nature Geoscience 12, 851–855.
Tagami, T., Nishimitsu, Y., Sherrod, D.R., 2003. Rejuvenated-stage volcanism after 0.6-m.y. quiescence at West Maui volcano, Hawaii: new evidence from K-Ar ages and chemistry of Lahaina Volcanics. J. Volcanol. Geother. Res. 120, 207–214.
Tanaka, R., Nakamura, E., Takahashi, E., 2002. Geochemical Evolution of Koolau Volcano, Hawaii. In: Takahashi, E., Lipman, P.W., Garcia, M.O., Naka, J., Aramaki, S. (Eds.), Hawaiian Volcanoes: Deep Underwater Perspectives. American Geophysical Union, pp. 311–332 Geophys. Monogr. Ser. 128.
Tanaka, R., Makishima, A., Nakamura, E., 2008. Hawaiian double volcanic chain triggered by and episodic involvement of recycled material: constraints from temporal Sr-Nd-Hf-Pb isotopic trend of the Loa-type volcanoes. Earth Planet. Sci. Lett. 265, 450–465.
Tatsumoto, M., 1978. Isotopic composition of lead in oceanic island basalts and its implication to mantle evolution. Earth Planet. Sci. Lett. 38, 63–87.
Taylor, B., 2006. The single largest oceanic plateau: Ontong Java-Manihiki-Hikurangi. Earth Planet. Sci. Lett. 241, 372–380.
Thomson, A.R., Crichton, W.A., Brodholt, J.P., Wood, I.G., Siersch, N.C., Muir, J.M.R., Dobson, D.P., Hunt, S.A., 2019. Seismic velocities of $CaSiO_3$ perovskite can explain LLSVPs in Earth's lower mantle. Nature 572, 643–647.
Tree, J.P., 2016. Mantle potential temperatures of 4.5 to 47 Ma Hawaiian volcanoes using olivine thermometry: Implications for melt flux variations. M.Sc. Thesis. University of Hawai'i at Mānoa, Honolulu.
Van Ark, E., Lin, J., 2004. Time variation in igneous volume flux of the Hawaii-Emperor hot spot seamount chain. J. Geophys. Res. 109, B11401.
Verzhbitskii, E.V., Lobkovskii, L.I., Kononov, M.V., Kotelkin, V.D., 2006. Genesis of Shatsky and Hess Oceanic rises in the Pacific Ocean as deduced from geologic-geophysical data and numerical modeling. Geotectonics 40 (3), 236–245.
Vidal, V., Bonneville, A., 2004. Variations of the Hawaiian hot spot activity revealed by variations in the magma production rate. J. Geophys. Res. 109, B03104.
Vlastélic, I., Dosso, L., 2005. Initiation of a plume-ridge interaction in the South Pacific recorded by high-precision Pb isotopes along Hollister Ridge. Geochem. Geophys. Geosyst. 6 (5), Q05011.
Warren, J.M., 2016. Global variations in abyssal peridotite compositions. Lithos 248-251, 193–219.
Warren, J.M., Shimizu, N., Dick, H.J.B., Nakamura, E., 2009. An assessment of upper mantle heterogeneity based on abyssal peridotite isotopic compositions. J. Geophys. Res. 114, B12203.
Weis, D., Frey, F.A., 2002. Submarine basalts of the Northern Kerguelen Plateau: interaction between the Kerguelen plume and the Southeast Indian Ridge revealed at ODP Site 1140. J. Petrol. 43 (7), 1287–1309.
Weis, D., Kieffer, B., Maerschalk, C., Pretorius, W., Barling, J., 2005. High-precision Pb-Sr-Nd-Hf isotopic characterization of USGS BHVO-1 and BHVO-2 reference materials. Geochem. Geophys. Geosyst. 6, Q02002.
Weis, D., Kieffer, B., Maerschalk, C., Barling, J., De Jong, J., Williams, G.A., Hanano, D., Pretorius, W., Mattielli, N., Scoates, J.S., Goolaerts, A., Friedman, R.M., Mahoney, J.B., 2006. High-precision isotopic characterization of USGS reference materials by TIMS and MC-ICP-MS. Geochem. Geophys. Geosyst. 7, Q08006.
Weis, D., Kieffer, B., Hanano, D., Nobre Silva, I., Barling, J., Pretorius, W., Maerschalk, C., Mattielli, N., 2007. Hf isotope compositions of U.S. Geological Survey reference materials. Geochem. Geophys. Geosyst. 8 (6), Q06006.
Weis, D., Garcia, M.O., Rhodes, J.M., Jellinek, M., Scoates, J.S., 2011. Role of the deep mantle in generating the compositional asymmetry of the Hawaiian mantle plume. Nat. Geosci. 4, 831–838.
Weis, D., Harrison, L.N., McMillian, R., Garcia, M.O., 2019. Basalt geochemistry reveals Hawaiian mantle plume and Earth's deep mantle fine structure. submitted. .
Wendt, J.I., Regelous, M., Nou, Y., Hékinian, R., Collerson, K.D., 1999. Geochemistry of lavas from the Garrett Transform Fault: insights into mantle heterogeneity beneath the eastern Pacific. Earth Planet. Sci. Lett. 173, 271–284.
Wessel, P., 2016. Regional-residual separation of bathymetry and revised estimates of Hawaii plume flux. Geophys. J. 204, 932–947.
White, R.S., 1993. Melt production rates in mantle plumes. Philos. Trans. R. Soc. Lond. A 342, 137–153.
White, W.M., 2015a. Isotopes, DUPAL, LLSVPs, and Anekantavada. Chem. Geol. 419, 10–28.
White, W.M., 2015b. Probing the Earth's deep interior through geochemistry. Geochem. Persp. 4 (2), 95–251.
White, W.M., Duncan, R.A., 1996. Geochemistry and geochronology of the Society Islands: New evidence for deep mantle recycling. In: Basu, A., Hart, S. (Eds.), Earth Processes: Reading the Isotopic Code, pp. 183–206 Geophys. Monogr. Ser. 95.
Whittaker, J.M., Afonso, J.C., Masterton, S., Muller, R.D., Wessel, P., Williams, S.E., Seton, M., 2015. Long-term interaction between mid-ocean ridges and mantle plumes. Nat. Geosci. 8, 479–484.
Williamson, N.W., Weis, D., Scoates, J., Pelletier, H., Garcia, M.O., 2019. Tracking the geochemical transition between the Kea-dominated Northwest Hawaiian Ridge and the bilateral Loa-Kea trends of the Hawaiian Islands. Geochem. Geophys. Geosyst. 20 (9), 4354–4369. https://doi.org/10.1029/2019GC008451.
Wolff, J.A., Palacz, Z.A., 1989. Lead isotope and trace element variation in Tenerife pumices: Evidence for recycling within an ocean island volcano. Mineral. Mag. 53 (373), 519–525.
Woodhead, J.D., 1992. Temporal geochemical evolution in oceanic intra-plate volcanics: a case study from the Marquesas (French Polynesia) and comparison with other hotspots. Contrib. Min. Petrol. 111, 458–467.
Woods, M.T., Davies, G.F., 1982. Late Cretaceous genesis of the Kula Plate. Earth Planet. Sci. Lett. 58 (2), 61–166.
Workman, R.K., Hart, S.R., Jackson, M., Regelous, M., Farley, K.A., Blusztajn, J., Kurz, M.D., Staudigel, H., 2004. Recycled metasomatized lithosphere as the origin of the enriched mantle II (EM2) end-member: evidence from the Samoan volcanic chain. Geochem. Geophys. Geosyst. 5, 2003gc000623.
Wright, N.M., Seton, M., Williams, S.E., Müller, R.D., 2016. The Late Cretaceous to recent tectonic history of the Pacific Ocean basin. Earth Sci. Rev. 154, 138–173.
Xu, G., Frey, F.A., Clague, D.A., Weis, D., Beeson, M., 2005. East Molokai and other Kea-trend volcanoes: magmatic processes and sources as they migrate away from the Hawaiian hot spot. Geochem. Geophys. Geosyst. 6, Q05008.
Xu, G., Frey, F.A., Clague, D.A., Abouchami, W., Blichert-Toft, J., Cousens, B., Weisler, M., 2007. Geochemical characteristics of West Molokai shield- and postshield-stage lavas: constraints on Hawaiian plume models. Geochem. Geophys. Geosyst. 8, Q08G21.
Yang, H.-J., Frey, F.A., Clague, D.A., 2003. Constraints on the source components of lavas forming the Hawaiian North Arch and Honolulu Volcanics. J. Petrol. 44 (4), 603–627.
Zindler, A., Hart, S., 1986. Chemical geodynamics. Ann. Rev. Earth Planet. Sci. 14, 493–571.